Understanding the functional of SAM and SH3 domain containing adaptor protein 1, SASH1

by

Angela Hussainkhel

B.Sc., Simon Fraser University, 2008

A THESIS SUBMITTED IN PARTIAL FULFILLMENT OF

THE REQUIREMENTS FOR THE DEGREE OF

MASTER OF SCIENCE

in

The Faculty of Graduate Studies

(Interdisciplinary Oncology)

THE UNIVERSITY OF BRITISH COLUMBIA

(Vancouver)

August 2012

ABSTRACT

TLR4 is the most extensively studied of TLR pathways in innate immune signaling that provides the first line of defense against invading pathogens. SASH1, a large protein composed of SAM and SH3 domain, is a novel positive regulator of the pathway in endothelial cells. SASH1 acts as a scaffold protein in the TLR4 pathway by independently binding TRAF6/TAK1/ IKKβ/IKKα and regulating TRAF6 and TAK1 ubiquitination leading to LPS-induced activation of NF-κB resulting in production of pro-inflammatory cytokines. To investigate SASH1 *in vivo* function, SASH1 gene-trap mice were generated. These mice have a β-galactosidase reportor construct insterted into intron 14-15 resulting in a truncation of the SH3 domain, and thereby loss of the two SAM domains and TRAF6 binding motif. However, SASH1 gene-trap mice do not provide any viable homozygous adults . X-gal staining of the heterozygous SASH1 adult tissues demonstrated SASH1 transcripts to be predominantly expressed in microvascular endothelium. This thesis is the continuation of the above findings to further characterize the role of SASH1 *in vitro* and *in vivo*. Work presented here confirms the role of SASH1 as a positive regulator of the TLR4 pathway by promoting activation of NF-κB. SASH1 does not interact with the E2 ligases and IKKγ. These results further elucidate a model for SASH1 in the TLR4 pathway where the E2 ligases and IKKγ are incorporated into a complex through interaction with proteins that are assembled by SASH1 to promote the downstream signaling. SASH1 homozygous gene-trap mice die in the perinatal period and preliminary analysis shows the lung as the potential organ being affected by SASH1 disruption. Homozygous gene-trap lungs appear deflated, sink in PBS and have smaller airways compared to wild-type control. However, morphometric analysis of the lung is still required to conclusively define a lung defect. In addition, I generated SASH1-floxed embryonic stem cells to be used for generating mice with a conditionally targeted allele of

SASH1 in endothelial cells to study the role of SASH1 in the endothelial response to LPS in

TLR4 signaling *in vivo,* hence contributing to the field of innate immune signaling.

PREFACE

The work pertaining to the identification of SASH1 as a novel TLR4 signaling molecule in endothelial cells presented in Introduction and at the beginning of Chapter 3 is unpublished, but the manuscript has been written and submitted. Shauna Dauphinee, a former PhD student, identified SASH1 as a novel regulator in TLR4 pathway and characterized its role as a scaffold protein that assembles signaling molecules downstream of the receptor. She also generated SASH1 gene-trap mice. I helped by performing coimmunoprecipitation and Western blot analysis for interaction of SASH1 with Uev1A, Ubc13 and IKKγ and by generating SASH1 lentiviral mediated knockdown cells to confirm the decrease in NF-κB activation by performing NF-κB luciferase assay and IκBα degradation Western blot analysis. In addition, I helped by designing the genotyping strategy and genotyping SASH1 gene-trap mice, performing RT-qPCR, β-galactosidase staining of SASH1 heterozygous gene-trap adult tissues and characterizing SASH1 gene-trap mice lethality stage. Here I also show a preliminary analysis of the cause of SASH1 gene-trap mice death. Shauna Dauphinee wrote the manuscript that was reviewed by Aly Karsan. The rest of the Chapter 3 and all of Chapter 4 was conceptualized by me and Aly Karsan and performed by me.

Experiments presented in this thesis are approved by UBC animal care and ethics committee (A10-0121 - Lipopolysaccharide Signaling in the Vasculature and A07-0717 - Endothelial to Mesenchymal Transformation) and the biohazard work was conducted in accordance to UBC biosafety guidelines.

TABLE OF CONTENTS

LIST OF TABLES

LIST OF FIGURES

LIST OF ABBREVIATIONS

DD, death domain

DMEM, dulbecco modified eagle media

E18.5, embryonic day 18.5

EC, endothelial cells

ESC, embryonic stem cells

FADD, fas associated death domain

FBS, fetal bovine serum

FCS, fetal calf serum

FGF, fibroblast growth factor

GAPDH, glyceraldehyde 3-phosphate dehydrogenase

HMEC, human microvessel endothelial cells

IB, immunoblot

IFNβ, interferon β

Ig, immunoglobulin

IL-6, interleukin 6

IP-10, interferon gamma inducible protein

IP: immunoprecipitation

IκB, inhibitor of nuclear transcription factor-κB

IKK, inhibitor of nuclear transcription factor- κB kinase

IRAK, interleukin-1 receptor associated kinase

IRF, interferon regulatory factor

ISRE, interferon stimulated response element

JNK, c-jun NH2-terminal kinase

K63, lysine 63

LBP, lipopolysaccharide binding protein

LOH, loss of heterozygosity

LPS, lipopolysaccaride

LRR, leucine-rich repeat

MAPK, mitogen activated protein kinase

MEF, mouse embryonic fibroblast

MyD88, myeloid differentiation factor 88

NFκB, nuclear transcription factor-κB

NO, nitric oxide

ORF, open reading frame

PAMP, pathogen associated molecular pattern

PBS, phosphate buffered saline

PFA, paraformaldehyde

RT-qPCR, reverse transcriptase-quantitative polymerase chain reaction

SAM, sterile α motif

SASH1, SAM and SH3 domain containing protein 1

SDS, sodium dodecyl sulfate

SH3, Src homology 3

SLY1, Src homology 3 domain expressed in lymphocytes

Src, V-Src avaian sarcoma viral oncogene

TAB, transforming growth factor-β-activated kinase 1-binding protein

TAK1, transforming growth factor-β-activated kinase 1

TBK1, tumor necrosis factor receptor associated factor family member-associated nuclear transcription factor- κB activator binding kinase 1

TGF-β, transforming growth factor- β

TIR, Toll/interleukin-1 receptor

TIRAP, TIR domain-containing adaptor protein

TLR, Toll-like receptor

TNF α, tumor necrosis factor α

TRAF6, tumor necrosis factor receptor associated factor 6

TRAM, Toll/interleukin-1 receptor-containing adaptor inducing interferon β-related adaptor molecule

TRIF, Toll/interleukin-1 receptor-containing adaptor inducing interferon β

TSG, tumor suppressor gene

Uev1A, ubiquitin-conjugating enzyme E2 variant

Ubc13, ubiquitin-conjugating enzyme 13

VCAM-1, vascular cell adhesion molecule

VEGF, Vascular endothelial growth factor

ACKNOWLEDGEMENTS

CHAPTER 1: INTRODUCTION

1.1 INTRODUCTION

The innate immune system is the first line of defense against invading pathogens. It uses a diversity of receptors to recognize and respond to pathogens. One such family of receptors, known as Toll-like receptors (TLR), recognizes conserved microbial motifs that are not found in mammals. To date, 11 TLR have been described in humans and 13 in mice. TLR4 is the most extensively studied of the TLR pathways. We recently discovered that SASH1, SAM and SH3 domain containing adaptor protein1, acts as a scaffold protein by assembling signaling molecules to promote TLR4 pathway in endothelial cells. SASH1 is a large protein with two SAM domains, a SH3 domain and a TRAF6 binding motif. To understand the *in vivo* function of SASH1, gene-trap mice were generated. The insertion of the gene-trap construct results in truncation of the SH3 domain, and thereby loss of the two SAM domains and the TRAF6 binding motif. However, SASH1 gene-trap mice do not produce any viable homozygous adults and die in the perinatal period. Preliminary analysis indicates the lung as the potential organ being affected by SASH1 disruption. In addition, X-gal staining of the heterozygous SASH1 adult tissues demonstrated SASH1 transcripts to be primarily expressed in microvascular endothelium. Therefore, to understand the role of SASH1 in endothelial TLR4 responses to LPS *in vivo,* we began generating SASH1 floxed embryonic stem cells to generate endothelial specific SASH1^{null} mice.

In this chapter, I will provide background on the innate immune system, endothelial cells and their role in innate immunity as well as background on TLRs particularly focusing on the TLR4 signaling pathway. Since we found SASH1 gene-trap pups to potentially have a lung defect, I will also provide background on the role of endothelial cells in lung development and on lung development itself.

2

1.2 THE IMMUNE SYSTEM

The immune system is a complex network of cells, tissues, organs and processes that work together to protect an organism against invading pathogens by distinguishing self from non-self. The immune system is divided into two classes - innate response and adaptive response. The innate immune response provides a non-specific immediate defense against invading pathogens, but it does not confer long-lasting immunity to the host. In contrast, the delayed antigen-specific adaptive immune response provides the immune system with the ability to recognize pathogens and create immunological memory so that a subsequent exposure to the same antigen will elicit a stronger response [1].

The innate immune system is the host's first line of defense against invading pathogens. It is evolutionarily conserved and present at birth. Mechanisms through which innate immunity act include: physical barriers, physiological barriers, phagocytic or cellular barriers and inflammatory barriers [2]. The physical barrier is comprised of skin and mucus membranes. The skin acts by having thick keratinized layer that is impermeable to most pathogens. The mucus membranes, that line the internal tracts of the body exposed to external environment, also provide protection from infection. Underneath the mucus, the epithelial cells are covered with cilia that sweep away invading pathogens [3]. Physiological barriers of innate immunity include temperature, pH, and the presence of normal microflora in the gastrointestinal tract and skin and production of various antimicrobial substances, such as complement. Complement, a group of serum proteins activated by bacterial products, plays an important role in pathogen destruction and clearance by activating an enzymatic cascade [4]. Once pathogens penetrate through physical and physiological barriers, specialized cells called phagocytes function to prevent infection. In the process of phagocytosis, pathogenic microbes are recognized by cell surface

receptors that initiate a signaling cascade in the engulfing cells leading to uptake and delivery of pathogen to lysosome for destruction [5, 6]. The last innate immune barrier to infection is inflammation characterized by redness, tumor, heat and pain. During inflammation, proinflammatory mediators cause the recruitment of immune cells to the site of infection from blood and neutrophil degranulation and subsequent tissue damage [6]. If the barriers of the innate immune system are not able to prevent pathogen invasion, the host will initiate an adaptive immune response.

1.3 ENDOTHELIAL CELLS AND THEIR ROLE IN INNATE IMMUNITY

The vasculature is an arrangement of blood vessels that distributes oxygen and nutrients throughout the body. Endothelial cells line the inner walls of blood vessels. The endothelium is composed of almost 10^{13} cells [7]. Among other functions, the endothelium acts to maintain organ homeostasis including vasoregulation, vascular permeability and providing an anti-coagulant surface [8]. It also regulates cellular and nutrient trafficking, participates in making new blood vessels and contributes to local balance of pro- and anti-inflammatory mediators [9]. Under normal conditions, endothelial cells sense and respond to changes in the extracellular environment. However, during infection the regulated physiological balance is disturbed resulting in endothelial dysfunction and injury and if left untreated can lead to sepsis [9]. However, it is not clear whether the endothelial dysfunction is a direct consequence of bacterial product interaction with endothelium or a secondary effect of inflammatory mediators produced by immune cells.

Sepsis is the systemic hyper-inflammatory response to bacterial infection, which is characterized by an initial hyperinflammatory response followed by a prolonged immunosuppressive state [10]. It is the leading cause of death in critically ill patients. In sepsis,

dysregulation of the immune response leads to excessive production of various pro-and anti-inflammatory cytokines and cellular injury resulting in multiple organ failure, coagulation disorders and in some cases death [10]. Research has shown that when receptors on immune cells and endothelial cells sense bacterial products, signal transduction cascades are activated that lead to activation of transcription factors such as nuclear transcription factor-κB (NF-κB) and interferon regulatory factor (IRF) resulting in production of pro-inflammatory cytokines [8]. Inhibition of NF-κB specifically in endothelium improves survival following bacterial infection and sepsis [11].

The endothelium plays an important role in mediating the early hyperinflammatory response in sepsis by releasing inflammatory mediators, recruiting leukocytes and facilitating their transmigration into tissue and promoting coagulation [9, 12]. Endothelial cells, like immune cells, have cell surface receptors that recognize bacterial components during microbial invasion and infection to activate the innate immune response. One such bacterial component is lipopolysaccharide (LPS) , which is a component of the Gram negative bacterial cell wall and a potent endotoxin [8]. The endothelial cell response to LPS includes actin reorganization, breaching of the endothelial cell barrier and cell detachment from the underlying matrix [13]. LPS can directly disrupt endothelial cell monolayer integrity through caspase cleavage of adherens junction proteins [13]. Thus, endothelial cells play a pivotal role in the innate immune response.

1.4 LUNG DEVELOPMENT

Development of the lungs begins with endodermal budding from the ventral foregut at around 4 to 6 weeks of gestation in humans and on embryonic day (E) 9.5 in mice (9) [14]. The buds undergo rounds of branching to give rise to airways. Branching morphogenesis of the left

5

and right bronchi to form lobular branches extends up to about 20 weeks of gestation in humans, while branching in mice happens at around E 11.5 to E17.5 [14]. Alveolarization begins at about 20 weeks of gestation in humans and continues to 7 years of age while in mice the differentiation phase encompassing alveolarization starts at E18.5 to postnatal day (P) 0 [14]. In the mature lung, large pulmonary vessels branch with the airways and capillaries form an intimate association with the alveolar epithelium. The arrangement in the lungs allows for gas exchange. In *utero*, the lung is a hydraulic, fluid-filled system. After birth, the umbilical cord clamping and a rush of catecholamines causes the lung lumen to dry out and the lung rapidly switches to air breathing [14, 15].

While the airways are made up of epithelial cells, the mesenchyme surrounding the epithelial cells gives rise to different cell types such as blood vessels, interstitial cells and smooth muscle cells of the upper airways [16]. Normal lung development depends on interactive signaling between the epithelial cells and mesenchymal cells of the lungs. Hence, the development of both airways and blood vessels is tightly coordinated. The mesenchymal cells produce important growth factors required for epithelial cell development. For example, the fibroblast growth factor 10- (FGF10-) null mutation in mice completely abolishes lung branching morphogenesis, while hypomorphic or ectopic FGF signaling results in a lethal neonatal alveolar defect [14, 16]. In turn, the epithelium produces molecules important for mesenchymal proliferation and differentiation such as Sonic hedgehog (Shh) and Bone morphogenetic protein 4 (BMP4).

Pulmonary surfactant, which is composed of a lipoprotein complex formed by type II alveolar cells, is essential for normal pulmonary function. It serves to decrease surface tension of the alveolar air-liquid interface preventing pulmonary collapse upon exhalation. Surfactant is particularly important during delivery as it allows lungs to be cleared of amniotic fluid and to be

filled with air. Surfactant deficiency and decreased function can cause respiratory distress syndrome in pre-term newborns. Respiratory distress syndrome is one of the main causes of the respiratory mortality in newborns [17].

1.5 ENDOTHELIAL CELL ROLE IN LUNG DEVELOPMENT

The endothelium plays a critical active role in perinatal lung development. Endothelial cells in the mesenchyme give rise to blood vessels that are an integral component of the lung. The epithelial cells gives rise to airways. In the mature lungs, blood vessels and airways form close associations with each other as blood vessels branch along with airways, and capillaries surround the alveolae sacs for gas exchange purposes [15, 16, 18]. During lung development, blood vessels form either by vasculogenesis or angiogenesis. Vasculogenesis is the development of blood vessels *de novo* from endothelial cells in the mesenchyme, while angiogenesis is the sprouting of new vessels from existing ones [18]. Vascular endothelial growth factor (VEGF) is a potent endothelial cell growth factor affecting both angiogenesis and vasculogenesis in a dose-dependent manner [19] . Deletion of one allele of the VEGF gene leads to embryonic lethality due to impaired vessel formation, delayed endothelial cell development and vessel sprouting [19].

Vascular development is tightly correlated with airway development for establishment of a set of functional lungs. Inhibition of vascular development with antisense oligonucleotides targeted against VEGF results in striking abolishment of epithelial airway branching morphogenesis and maturation [18]. Tight coordination and regulation between endothelium and epithelium in lung is also suggested by the pattern of expression of VEGF specifically on epithelial cells during embryonic lung development and VEGF receptors on endothelial cells [19].

Once the vessel is formed, endothelial cells express and secrete factors to regulate vascular growth and maturation. Before birth, alveoli are filled with fluid and pulmonary vascular resistance (PVR) is high [14, 15]. At this time endothelial cells secrete more vasoconstrictors than vasodilators. However, immediately after birth, the lungs change to an air-breathing organ. One of the main functions of endothelial cells is to help reduce PVR allowing blood to pass through the lungs for the first time at birth and to help clear alveolar fluid [15]. Endothelial cells go through structural and functional changes for oxygenation to occur immediately after birth. Endothelial structural remodelling is evident minutes after birth when endothelial cells become thinner and the vessel lumen expands. The physiological changes following increased oxygen tension and blood flow constitute activation of vasodilators such as nitrogen oxide and bradykinin that result in relaxation of blood vessels [15].

1.6 TOLL-LIKE RECEPTORS

TOLL-Like Receptors (TLR) are transmembrane proteins that are evolutionary conserved between humans and insects. Toll receptors were initially identified in Drosophila to be essential for establishing dorso-ventral polarity during embryogenesis [20, 21]. Toll mutant flies were then found to be more susceptible to fungal infection [20]. Subsequently, mammalian homologues of Toll receptors were identied and called Toll-like receptors (TLR) [19]. Toll proteins play an important role in innate immunity by recognizing conserved microbial motifs, pathogen-associated molecular pattern (PAMPs) that are not found in mammals [21]. To date 11 TLR described in humans and 13 in mice have been identified [22-24]. TLRs induce signaling pathways which result in production of pro-inflammatory cytokines such as IL-6, IFN, TNF and IL-12 [10]. TLRs have an extracellular domain and a cytoplasmic tail that contains a conserved region called the Toll/IL-1 receptor (TIR) domain. The subcellular localization of TLR to some

extent correlates to the type of ligand they bind to. TLR3, TLR7, TLR8, TLR9 are localized in the endosomal compartment while TLR1, TLR4, TLR5, TLR6, TLR10 are localized on the cell surface (Figure 1.1) [25]. TLRs bind to components of bacterial, viral, fungal and protozoal origin. TLR1, TLR2 and TLR6 detect lipopeptides while TLR3, TLR7, TLR8 and TLR9 recognize nucleic acids [26-28] . TLR5 detects flagellin while TLR4 recognizes lipopolysaccharides (LPS) [28, 29]. Table 1.1 shows a list of TLR ligands. Besides the exogenous ligands, TLRs also get activated by endogenous ligands such as heat shock proteins 60 (hsp), fibrinogen, surfactant protein, fibronectin extra domain A Recombinant product, heparan sulfate and soluble hyaluronan [28]. Other than TLR3, the TLRs share a common signaling pathway via the adaptor molecule MyD88, which has a TIR domain in its C-termianl region and a death domain (DD) in its N-terminal region [20, 21].
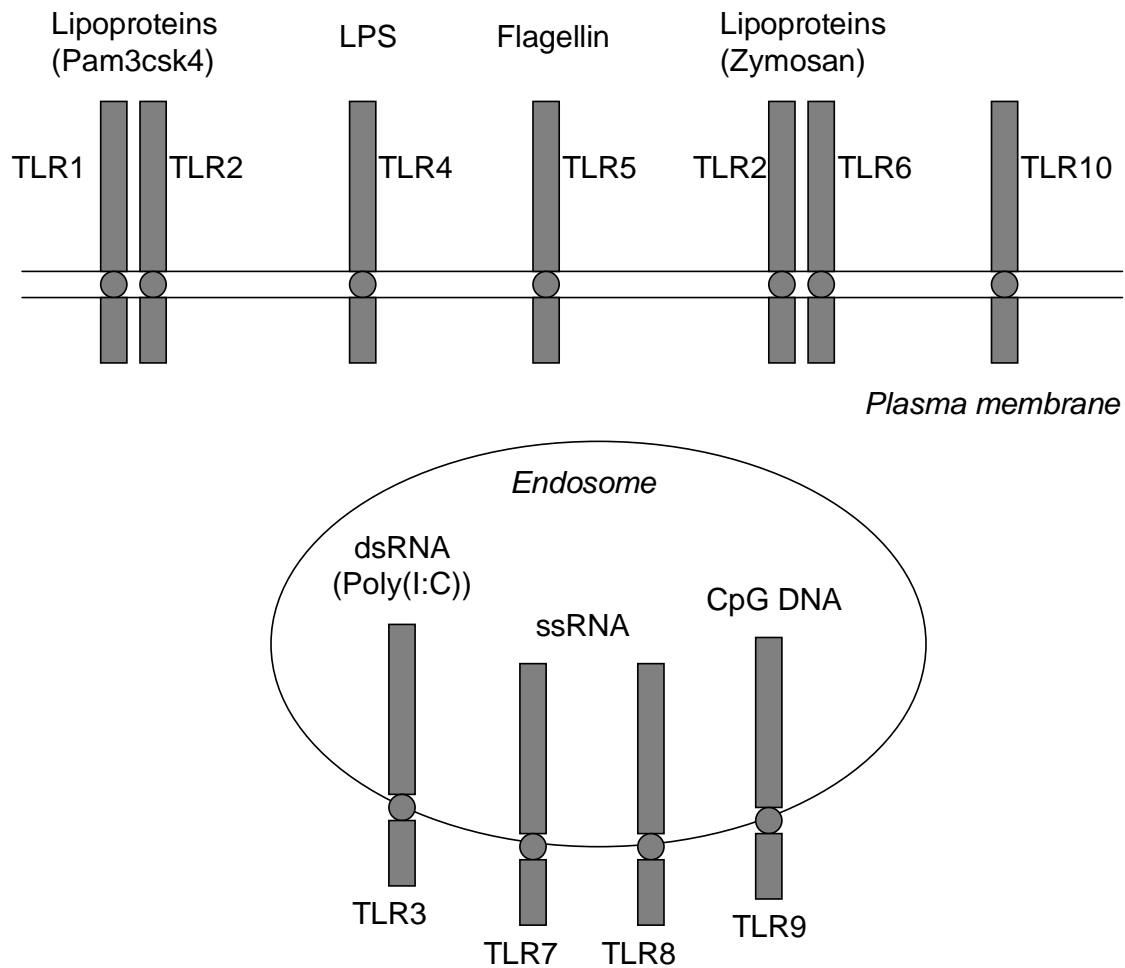
Figure 1.1 Cellular localization of TLRs

TLR1/2, TLR4, TLR5, TLR2/6 and TLR10 are found on the plasma membrane, while TLR3, TLR7, TLR8 and TLR9 are found in the endosome. The localization of TLR11, TLR12 and TLR13 is not known. There are 11 TLRs characterized in humans.

Table 1.1 TLR ligands found in human and mouse

Ligands of TLR1-13. TLR1-9 are found in both human and mouse. TLR10 is found in human only and TLR11-13 is found in mice only. Additional species and their TLRs are not shown since they are not relevant to this thesis.

Receptor	Ligand	Origin of Ligand
TLR1	Triacyl lipopeptides	Bacteria
TLR2	Lipoprotein/lipopeptide	various pathogens
	Peptidoglycan	bacteria
	Glycolipids	bacteria
	Lipoteichoic acid	Bacteria
	Zymosan	Fungi
	Heat-shock protein 70	Host
TLR3	Double-stranded RNA	Viruses
TLR4	Lipopolysaccharide	Bacteria
	Heat-shock proteins	bacteria and host
	Hyaluronic acid	host
	Fibrinogen	host
	heparan sulfate	host
TLR5	Flagellin	Bacteria
TLR6	Diacyl lipopeptides	Bacteria
	Lipoteichoic acid	Bacteria
	Zymosan	Fungi
TLR7	Single stranded RNA	Viruses
TLR8	Single stranded RNA	Viruses
TLR9	CpG-containing DNA	Bacteria and viruses
TLR10	unknown	unknown
TLR11	Profilin	Protozoa
TLR12	unknown	unknown
TLR13	unknown	unknown

1.7 TOLL LIKE RECEPTOR 4 (TLR4) SIGNALING PATHWAY

The innate immune response is initiated upon LPS binding to TLR4. LPS is a key component of the outer membrane of Gram-negative bacteria . It is also called endotoxin. LPS is a complex glycolipid composed of a hydrophilic polysaccharide and a hydrophobic domain, known as lipid A, which is responsible for the biological activity of LPS [8]. Binding of LPS to the endothelial cell surface provokes endothelial responses as exhibited by expression of proinflammatory cytokines and adhesion molecules [8]. LPS also activates immune cells to express proinflammatory cytokines that in turn regulate activation of endothelial cells.

TLR4 is the most extensively studied of TLRs. It was identified as the LPS signaling receptor by studies performed on the C3H/HeJ mutant mouse strain that has a missense point mutation within the cytoplasmic domain of the TLR4 receptor [30]. The mutant mice were shown to be hyporesponsive to LPS [30]. In addition, gene-targeted TLR4 mice were generated that were hyporesponsive to LPS confirming it to be the LPS receptor [30] .

LPS stimulates mammalian cells through a series of interactions with several proteins including the LPS binding protein (LBP), CD14, MD-2 and TLR4. LBP plasma concentration levels rise during inflammation. LBP is a soluble protein that directly binds to LPS and facilitates the interaction between LPS and CD14 [31]. In endothelial cells, LBP can also function to enhance LPS uptake [31]. CD14 exists in both a soluble proteolytic fragment form found in the serum (sCD14) or a membrane anchored glycosyl-phosphatidylinositol (GPI) protein on the cell surface (mCD14) [32]. CD14 functions in transferring LPS to the TLR4/MD-2 receptor complex and recognition of the LPS molecule itself [8]. Endothelial cells lack mCD14 so they require soluble CD14 that is present in plasma [33]. CD14 lacks an intracellular domain thus can not activate signaling by itself [32]. MD-2 is a soluble glycoprotein that non-covalently associates

with the ectodomain of TLR4 and directly binds LPS itself [8]. There is no evidence that LPS binds TLR4 directly, but TLR4 enchances binding of LPS to MD-2 [21]. TLR4 associates with its ligand and the co-receptors, CD14 and MD-2, by an extracellular domain made up of leucine-rich repeats (LRRs) [21]. LRRs are protein structural motifs that form horseshoe-like folds. They are composed of repeating amino-acid stretches that are usually rich in the hydrophobic amino acid leucine and mediate protein-protein interaction.

1.8 MYD88-DEPENDENT PATHWAY

Upon LPS stimulation, TLR4 undergoes oligomerization and recruites its downstream adaptors through interaction with the TIR (Toll-interleukin-1 receptor) domain [21]. The sequence of the TIR domain is highly conserved among species and within the TLR family [21].

IRAK was originally identified based on homology to Pelle, a kinase protein in the Toll pathway in *D. Melanogaster*. The IRAK family to-date consist of four members, IRAK1, IRAK2, IRAK4 and IRAKM [20, 21, 34]. The IRAK protein has an N-terminal death domain that interacts with MyD88 and a central kinase domain. IRAK1 and IRAK4 have serine/threonine kinase activity, while IRAK 2 and IRAKM are catalytically inactive [21] . IRAK4 has been shown to have an essential role in activation of the NF-κB pathway. IRAK4-deficient mice are resistant to lethal doses (40 mgkg^{-1} body weight) of LPS and IRAK4 deficient patients have impaired responses to microbial invasion [34]. However, RAK1-deficient macrophages are only partially impaired in producing proinflammatory cytokines. Thus, IRAK1 is only partially required for TLR signaling and selectively activates NF-κB [34]. While IRAK2 is also known to have a positive role in TLR signaling, IRAKM knock-out mice show an increased inflammatory response to bacterial infection demonstrating its negative inhibitory role in TLR signaling [20]. Upon recruitment to the receptor complex by MyD88, IRAK4

phosphorylates IRAK1 resulting in its auto and trans-phosphorylation and activation that results in dissociation from the receptor complex and association with Tumor Necrosis Factor (TNF) Receptor-Activated Factor 6 (TRAF6) [34].

TRAF6 belongs to a family of seven TRAF members that mediate signaling downstream of the TNF superfamily receptors (TNFR) [35]. All TRAF proteins except TRAF1 and TRAF7 have an N-terminal RING finger, several zinc fingers and a C-terminal TRAF domain [36]. The N-terminus acts as an E3 ubiquitin ligase and the C-terminal domain are responsible for interaction with TRAF proteins and other signaling proteins [37].

After IRAK1 is phosphorylated and activated it associates with TRAF6, and dissociates from the receptor forming a complex with transforming growth factor-β (TGF- β)-activated kinase 1 (TAK1) and TAK1 binding proteins, TAB1 and TAB2, at the membrane [8]. TAB1 functions as an activator of TAK1, while TAB2 and TAB3 bind polyubiquitin chains to link TAK1 to TRAF6 and mediate TRAF6 ubiquitination [38-40]. The complex of TRAF6, TAK1, TAB1 and TAB2 then moves into the cytoplasm, while IRAK1 stays in the membrane and is eventually degraded by the ubiquitin-proteosome system [8, 21]. TRAF6, TAK1, TAB1 and TAB2 protein assembly once in the cytoplasm forms a large complex with the E2 ubiquitin conjugating enzymes Ubc13 and Uev1A to catalyze the formation of a polyubiquitin chain linked through lysine 63 (K63) of ubiquitin on TRAF6 [8, 41, 42]. K63 linked polyubiquitin chains are important for signal transduction as opposed to the K48-linked polyubiquitin chain that target a protein for proteosomal degradation [42]. TRAF6 ubiquitination and activation then leads to activation of TAK1. Activated TAK1 then mediates phosphorylation of inhibitor of NF-κB (IκB) kinase (IKK) complex and the MAPK kinases (MKKs) [43]. The IKK complex is made up of two catalytic subunits and a regulatory subunit: IKKα, IKKβ and IKKγ (NEMO),

respectively [8, 21, 44]. Activated IKKs phosphorylate IκB family members resulting in degradation of of IκB proteins and the subsequent release and translocation of transcription factor NF-κB to the nucleus to activate expression of proinflammatory cytokines and other immunity-related genes [45].

TAK1 activation also leads to activation of the MAPK family involving p38 and c-jun NH2-terminal kinase (JNK) [8]. Like NF-κB, MAPK activation is still induced in MyD88-deficient macrophages implying MAPK are activated by both MyD88-dependent and - independent pathways. There is relatively less known about MAPK downstream of TLRs as opposed to NF-κB. Figure 1.2 shows a scheme of the TLR4 pathway.
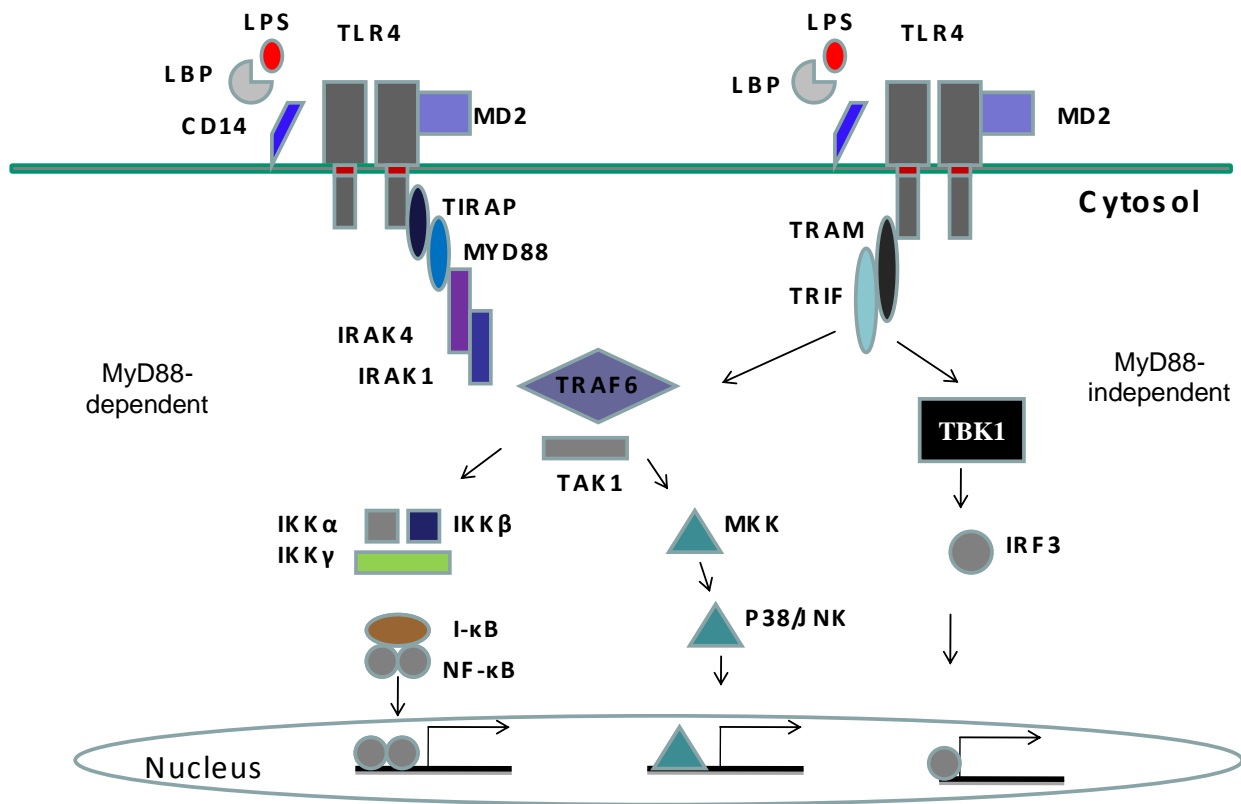
Figure 1.2 TLR4 signaling pathway

This figure shows both MyD88 dependent (left) and independent (right) pathway.

LPS binds to TLR4 receptor complex, resulting in recruitment of adaptor proteins. In MyD88-dependent pathway, IRAKs are recruited to the receptor complex. IRAK1 recruits TRAF6 culminating in activation of proinflammatory signaling pathways including NFκB and MAPKs. In MyD88-independent pathway, TRIF binds TRAF3 or TRAF6 leading to downstream activation of IRF3 or NFκB, respectively. LPS, lipopolysaccharide; TLR4, Toll-like receptor; TIRAP, toll-interacting protein; MyD88, myeloid differentiation factor 88; IRAK interleukin-1 receptor-associated kinase; TRAF6, tumor necrosis factor receptor associated factor-6; Ub, ubiquitin; TAB, transforming growth factor-β-activated kinase-1 binding protein; TAK1, transforming growth factor- β-activated kinase-1; NFκB, nuclear transcription factor-κB; IKK, IκB kinase; MKK, mitogen activated protein kinase kinase; JNK, c-jun NH2-terminal kinase; TRAM, Toll/interleukin-1 receptor containing adaptor inducing interferon β-related adaptor molecule; TRIF, Toll/interleukin-1 receptor-containing adaptor inducing interferon β; TBK1, TANK-binding kinase; IRF3, interferon regulator factor 3.

1.9 MYD88-INDEPENDENT PATHWAY

The MyD88-independent pathway was identified when MyD88 knock-out mice retained the ability to activate NF-κB and JNK with delayed kinetics [46]. However, MyD88 knock-out cells did not produce inflammatory cytokines [20]. LPS stimulation of MyD88 wild-type cells leads to expression of proinflammatory cytokines such as IL-6 and tumor necrosis factor α (TNF α) etc. On the other hand, analysis of MyD88 knock-out macrophages showed that LPS induction in these cells leads to expression of IFN-inducible genes such as IP-10 and IFN-γ through activation of transcription factor IRF-3 which in turn activates IFN-β [47, 48].

In the MyD88-independent pathway, upon LPS stimulation the adaptor protein TRAM is recruited to the cytoplasmic domain of TLR4 [8]. The receptor/adaptor complex translocates to the endosome where TRIF is recruited to the receptor complex [51] . TRIF is an important mediator of the MyD88-independent pathway as TRIF-deficient cells show impairment in activation of IRF3 and in late-phase activation of NF-κB [49]. TRIF functions in both TLR3 and TLR4 [49]. The recruitment of the adaptor proteins to the receptor complex results in binding of either TRAF6 or TRAF3 leading to late-phase activation of NF-κB or IFNβ, respectively [8, 50, 51]. TRAF3 associates with TRAF family member-associated NF-κB activator (TANK), TANK binding kinase 1 (TBK1) resulting in recruitment of the noncanonical IKK, IKKi, leading to phosphorylation and activation of IRF3 and in turn production of IFNβ [50].

1.10 NEGATIVE REGULATION OF TLR4 SIGNALING

Because the TLR4 signaling pathway leads to production of inflammatory cytokines that could result in sepsis, regulation of pathway is essential to protect the host from damage. The TLR4 signaling pathway, as would be expected, has many regulators [8]. Since discussing all of them is outside the scope of this thesis, I will describe some of the relevant ones.

17

1.10.1 Fas-associated death domain (FADD)

FADD is a proapoptotic adaptor protein that binds activated death receptors through its death domain (DD) to initiate apoptosis. FADD has been reported to negatively regulate TLR4 signaling. Our lab has shown that FADD inhibits TLR4 signaling by binding both IRAK1 and MyD88 and preventing their association [52]. This negative regulation by FADD results in decreased LPS-induced proinflammatory cytokine production.

1.10.2 A20

A20 is a zinc-finger protein that has been shown to have both ubiquitinating and deubiquitinating activites. A20 has been shown to be induced upon LPS stimulation to remove ubiquitin chains from TRAF6 resulting in inhibition of NF-κB activation and cytokine production [53]. A20 might provide a feedback inhibition mechanism in TLR4 signaling as A20-deficient macrophages show prolonged NF-κB activation and increased proinflammatory cytokine production [53].

1.10.3 β-arrestin

The arrestin family is comprised of four subtypes: the ubiquitiously expressed β-arrestin 1 and β-arrestin 2 and two arrestins exclusively expressed in retina of mammals [54]. In addition to their role in desensitisation and endocytosis of different cell surface receptors, β-arrestins are known for binding different cell signaling molecules and thus regulating signaling cascades. β -arrestin 1 and β-arrestin 2 have been reported to be essential negative regulators of TLR-IL-1R signaling. β-arrestin 2 deficient mice have enhanced proinflamatory cytokine expression in resonse to bacterial invasion and are more susceptible to endotoxic shock. β-arrestin 1 and β-arrestin 2 impart their inhibitory effect by binding TRAF6 and preventing its oligomerization and autoubiquitination and in turn inhibiting NF-κB activation [54].

1.11 SCAFFOLD PROTEINS IN IMMUNE SIGNALING

Signaling cascades require the interaction or proximity of different proteins and their proper localization in a specific compartment of the cell at a given time for the signal to get propagated from cell surface to the downstream effector molecules. This coordinated regulation is mediated by scaffold proteins. Scaffold proteins usually have many protein binding domains that allow them to bind multiple members of signaling cascade and assemble them into complexes. In doing so, scaffold proteins increase signal transduction specificity and efficiency. They regulate signal transduction by altering subcellular localization of the complex, coordinate positive and negative feedback or insulate the protein complex from inactivation of degradation [55].

TLR4 signaling has been extensively studied. However, not much is known about the role of scaffold proteins in the pathway.

1.12 SAM AND SH3 DOMAIN CONTAINING ADAPTOR PROTEIN 1 (SASH1)

SASH1 is a SAM and SH3 domain containing adaptor protein. It is found on chromosome 6.q24.3 and is made up of 20 exons [56]. SASH1 was originally identified by expression profiling and *in silico* analysis as a gene that is downregulated in breast and other solid cancers such as lung and thyroid [56]. Loss of heterozygosity (LOH) at 6q24.3 is associated with increased tumor size and poor prognosis [56]. In addition, SASH1 mRNA has been shown to be reduced in colon cancer and post-operative metastases in the liver [57]. These findings suggest SASH1 could act as a potential tumor suppressor gene (TSG). However, no functional studies have been done to prove the hypothesis.

It is ubiquitiously expressed in most human and mouse tissues. SASH1 encodes two transcripts of 4.4 and 7.5 kb due to two separate polyadenylation sequences [56]. The translation

start site resides in exon 1 and the stop codon exists in exon 20 followed by the polyadenylation signal. Alternatively, the 4.4 Kb transcrit with an expanded 3' UTR can be transcribed via use of a second polyadenylation signal. It is a large protein of 170 KDa comprised of 1247 amino acids. It contains two SAM domains and an SH3 domain. SAM domains are protein-protein interaction domains that can form homo- or heterooligomers with SAM domain-containing proteins and can even bind to non-SAM domain-containing proteins. SH3 domains also mediate protein-protein interactions through binding proline-rich sequences with a consensus motif of PXXP (where P is proline and X is any other amino acid). In our lab, we have also confirmed SASH1 to have a TRAF6 binding motif. Figure 1.3 shows SASH1 exons and domains.

SASH1 belongs to the family of SAM and SH3 family of adaptor proteins with SLY1 (SH3 domain expressed in lymphocytes) and SLY2/HACS1 (hemaptopoietic adaptor containing SH3 and SAM domain 1) as other members of the family [57]. SLY1 is implicated in regulating the adaptive immune response as SLY1 mutant mice have impaired lymphoid organ development and defects in humoral responses as well as impaired antigen receptor-mediated lymphocyte activation [58]. HACS1 is expressed in both normal and malignant hematopoietic cells and is upregulated in B cells [59] HACS1 mutants have increased adaptive immune responses [60] suggesting that both SLY1 and HACS1 play a role in addaptive immunity. Figure 1.4 shows all family members domain structure.
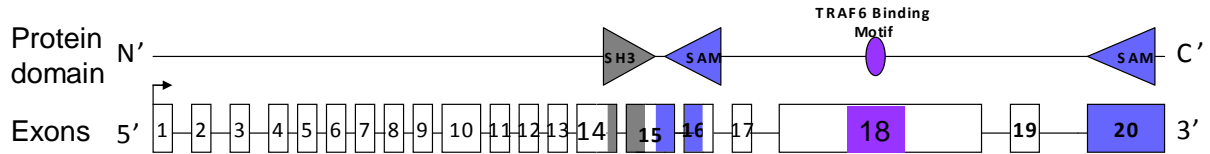
Figure 1.3 SASH1 structure

SASH1 has 20 exons. Translation start site (ATG) is located in exon 1 and stop codon is located in exon 20. SASH1 protein domain structure is shown at the top. The genomic location of protein domains is denoted. SH3, Src homology 3 domain; SAM, Sterile α motif.
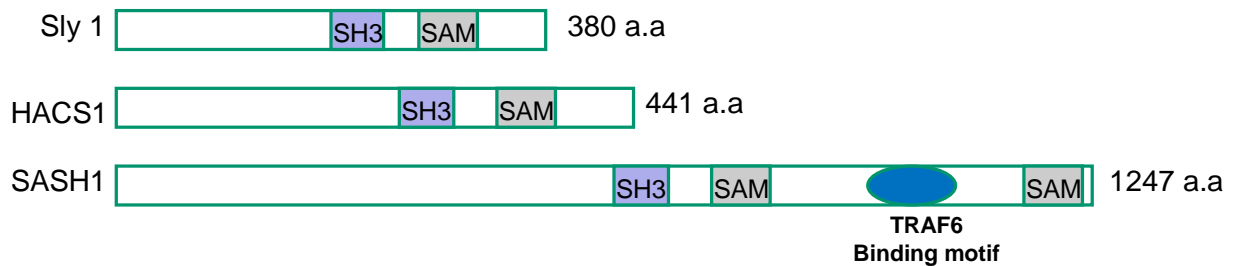
Figure 1.4 SAM and SH3 family of adaptor proteins

Domain structures of SAM and SH3 domain family of proteins. All three family members have only one SH3 domain. Sly1 and HACS1 have one SAM domain, while SASH1 has two SAM domains. SASH1 also has a TRAF6 binding motif. SH3, Src homology 3 domain; SAM, Sterile α motif; a.a, amino acid.

1.13 AIM OF THE CURRENT STUDY

Plasma membranes are lipid bilayers that contain specialized glycolipoprotein microdomains called lipid rafts, which function to cluster proteins and facilitate downstream signaling cascades. TLR4 signaling components have been shown to localize in lipid rafts after LPS stimulation [61]. FADD is a negative regulator of the TLR4 pathway in endothelial cells and in immune cells and FADD knock-out mouse embryonic fibroblasts (MEF) show increased activation in response to LPS [52]. The hyperactivation of the signaling pathway in FADD knock-out cells would facilitate detection and identification of a protein present in limiting amounts in the cells. Thus, our lab used FADD knock-out cells to identify novel proteins important for TLR4 signaling. Proteins from lipid microdomains from LPS-stimulated FADD-wild-type (WT) and FADD knock-out MEFs were isolated and mass spectrometric (MS) analysis was performed. Interestingly, SASH1 was detected in FADD knock-out cells and not FADD wild-type cells. Thus, this experiment identified SAM and SH3 containing protein (SASH1) as a putative candidate for positive regulation of the TLR4 pathway (Dauphinee et al., manuscript submitted). This formed the basis of the following studies in our lab to identify and investigate the role of SASH1 in TLR4 signaling.

Recent studies in our lab identified SASH1 to positively regulate TLR4 signaling in endothelial cells by increased activation of NF-κB and MAPK resulting in increased production of proinflammatory cytokines such as IL-6 and IP-10. Our lab also found SASH1 to interact with TRAF6 through a conserved TRAF6 binding motif and to regulate TRAF6 ubiquitination. SASH1 also independently binds TAK1, IKKβ and IKKα and regulates TAK1 ubiquitination (Dauphinee et al., manuscript submitted). Thus, we have found that SASH1 acts as a scaffold protein assembling signaling molecules downstream of TLR4 to activate early endothelial

responses against bacterial invasion. To investigate SASH1 *in vivo* function, SASH1 gene-trap mice were generated. These mice have a β-galactosidase reportor construct inserted into intron 14-15 resulting in a truncation of the SH3 domain, and thereby loss of the two SAM domains and TRAF6 binding motif. However, SASH1 gene-trap mice do not provide any viable homozygous adults. X-gal staining of the heterozygous SASH1 adult tissues demonstrated SASH1 transcripts to be primarily expressed in microvascular endothelium and parenchymal cells of several organs, but not in immune cells (Dauphinee et al., manuscript submitted)

This thesis is a continuation and addition to the recent findings in our lab that identified SASH1 as a novel regulator of TLR4 in endothelial cells. Experiments in the first part of this thesis confirm the role of SASH1 as a positive regulator of the pathway by promoting activation of the NF-κB transcription factor. We show that SASH1 does not interact with E2 ligases and IKKγ. Homozygosity for the *Sash1* gene-trap allele results in perinatal lethality and preliminary analysis indicates the lung as a potential organ being affected by SASH1 deficiency. In summary, the work in this thesis further characterizes the role of SASH1 *in vitro* in TLR4 signaling and *in vivo* using the gene-trap model. The work in the second part of this thesis generates SASH1-floxed embryonic stem cells (ESC), to be used for generating mice with a conditionally targeted allele of SASH1. Together, the work in this thesis furthers our understanding of the role of SASH1 as a scaffold protein in TLR4 signaling, begins characterizing SASH1 homozygous gene-trap mice, and begins the process of generating endothelial-specific SASH1-null mice to study the role of SASH1 in response to LPS hence contributing to the field of innate immune signaling.

CHAPTER 2: MATERIALS AND METHODS

2.1 MATERIALS

LPS was purchased from Sigma-Aldrich (St. Louis, MO). IκBα antibody was purchased from Santa Cruz Biotechnology Inc, CA; Tubulin antibody was purchased from Sigma-Aldrich, St. Louis, MO. PCR primers were ordered and obtained from IDT (Coralville, Iowa).

2.2 CELL CULTURE

The human microvascular endothelial cell line (HMEC) was provided by the Centers for Disease Control and Prevention (Atlanta, GA). HMEC lines were cultured in MCDB131 medium (Invitrogen, Carlsbad, CA) supplemented with 10% heat-inactivated fetal calf serum (FCS) (HyClone, Logan UT), 10 ng/mL epidermal growth factor (EGF) (Sigma-Aldrich, St. Louis, MO) 2 mM glutamine (Sigma-Aldrich, St. Louis, MO), and 100 U each of penicillin and streptomycin (Sigma-Aldrich, St. Louis, MO). HEK293T was cultured in Dulbecco modified Eagle medium (DMEM) (Invitrogen, Carlsbad, CA) supplemented with 10% heat-inactivated fetal bovine serum (FBS), 2 mM glutamine and 100 U each of penicillin and streptomycin (PSG). All cells were maintained at 37^0C in 5% CO_2.

2.3 RECOMBINANT PLASMID

SASH1 shRNA knockdown construct (RHS3979-98833405) and PLKO.1 vector control (RHS4533) were obtained from OpenBiosystems (Huntsville, AL). NF-κB Luc was a gift of F.R. Jirik, (University of Calgary, Calgary, AB). pFlox was obtained from Danny Chui (Genetic Modeling Core of the BCCA, Vancouver, BC). Genomic 129 bacterial artificial chromosome (BAC) was obtained from the Centre for Applied Genomics (Toronto, ON).

2.4 RNA INTERFERENCE

SASH1 knockdown (F1) and vector control PLKO.1 was purchased from OpenBiosystems (Huntsville, AL). HEK293T cells in 10 cm dishes were co-transduced with 6

μg shRNA vector, 3 μg pVSVG, 3 μg pMDL g/p PRE, and 3 μg RSV-REV using TransIT-siQUEST® transfection reagent according to the manufacturer's directions (Mirus Bio Corporation, Madison, WI) for production of lentiviral particles. Viral media were used to transduce target cells (HMEC) and positive cells were obtained by antibiotic selection.

2.5 LUCIFERASE ASSAY

HMEC cells were stably transduced with shSASH1 (F1) or vector control PLKO.1 and SASH1 knockdown was confirmed by qPCR. shSASH1 HMEC cells were seeded to a density of 50,000 cells per well. Transient transfection of luciferase assay constructs were performed after 24 h using Superfect transfection reagent (Qiagen, Mississauga, ON) according to the manufacturer's instructions. SASH1 knockdown cells were co-transfected with 300 ng of NF-κB luciferase reporter (pNF-κB-Luc) and a 7.5 ng of the Renil luciferase plasmid, pRL-CMV (Promega, Madison, WI, for pNF-κB-Luc) as an internal control. Before LPS stimulation (100 ng/mL) for 8 h, cells were serum-starved for 24 h post-transfection. After that, passive lysis was performed and luciferase activity was measured by dual luciferase assay (Promega, Madison, WI) on DLReady luminometer (Promega Corporation, Madison, WI).

2.6 PROTEIN ASSAY

Total protein concentration was assayed using the BioRad DC^{TM} Protein Assay Kit (BioRad Laboratories, Hercules, CA). Protein samples were diluted 5 times with distilled water and 5 μl of the sample was added to a dye solution containing 25 μl alkaline copper tartrate solution, 0.5 μl surfactant solution and 200 μl Folin reagent. Absorbance was measured at 560 nm after incubation at room temperature for 15 min. Protein concentration was determined against a standard curve of bovine serum albumin (BSA) at concentrations of 0, 0.125, 0.250, 0.5, 1 and 2 mg/mL.

2.7 IMMUNOBLOTTING

50 μg of protein was used for immunoblotting. Samples were diluted in SDS-PAGE sample buffer. The samples were boiled at 95^0C for 5 min for proteins denaturation and were loaded onto 10% acrylamide gels along with molecular weight markers. After SDS-PAGE, the proteins on the gel were transferred to nitrocellulose membranes (BioRad Laboratories, Hercules, CA) electronically for 45 min. Blots were then blocked in 5% skim milk powder (w/v) in Tris-buffered saline containing Tween-20 (TTBS; M Tris-HCL, pH, NaCl, and 0.05% Tween-20) for 1 h at room temperature. After that, the blots were incubated in the desired primary antibody overnight at 4^0C in 5% skim milk TTBS. The primary antibody concentration were as follows: IκBα (1:1000) from Santa Cruz Biotechnology Inc, CA, Tubulin (1: 50, 000) from Sigma-Aldrich, St. Louis, MO. After primary antibody incubation, blots were washed three times with TTBS for 15 min and then incubated with appropriate secondary antibody (1:5000, HRP-conjugated IgG, Sigma-Aldrich, St. Louis, MO) in 5% skim milk-TTBS for 1 h. After that, the blots were washed three times with TTBS for 10 min each. Then blots were incubated for 1 min in 1:1 mixture of enhanced chemiluminescence (ECL) reagents (PerkinElmer Life Sciences, Boston, MA). The membranes were blotted on Whatman paper and wrapped in plastic wrap before autoradiography.

2.8 CO-IMMUNOPRECIPITATION

TransIT-siQUEST® transfection reagent (Mirus Bio Corporation, Madison, WI) was used to co-transfect HEK293T cells with 5 μg of each expression plasmid according to manufacturer's instructions. Cell lysates were collected using modified RIPA buffer (50 mM Tris-HCl, pH 7.4, 150 mM NaCl, 1 mM EDTA, 1% NP-40, 0.25 % sodium deoxycholate plus protease inhibitors) after 48 hours. 1 mg of protein was first precleared by incubation with

agarose beads for 1 h and then incubated overnight with either anti-FlagM2-agarose beads or control IgG-agarose beads (Sigma-Aldrich, St. Louis, MO). Immunoprecipitation was also performed with anti-HA (1 μg) or anti-Myc (1 μg) overnight followed by incubation with protein G agarose beads (Cell Signaling Technologies, Danvers, MA) for an additional 24 h. Finally, the beads were washed three times in lysis buffer and boiled in SDS-PAGE sample buffer for immunoblot analysis.

2.9 RNA ISOLATION

Total RNA was isolated from cultured *in vitro* or tissues *in vivo* using TRIZOL® following manufacturer's instructions (Invitrogen, Carlsbad, CA). Total RNA concentration was measured by Nanodrop spectrophotometer.

2.10 QUANTITATIVE REVERSE TRANSCRIPTION POLYMERASE CHAIN REACTION (RT-QPCR)

Total RNA was extracted and cDNA was synthesized using 2.5 μg total RNA. DNA contamination was eliminated by DNase (Invitrogen, Carlsbad, CA). First strand cDNA synthesis was carried out using random priming (Invitrogen, Carlsbad, CA) and Superscript® II reverse transcriptase (Invitrogen, Carlsbad, CA). Samples were then amplified by real-time qPCR using 1 μM of forward and reverse primer mix and 7.5 μL of Fast Start Universal Sybergreen Master mix (Roche, Laval, QC). GAPDH was used as housekeeping gene. Primers are listed in the table 2.1. qPCR was performed using ABI Prism (Applied Biosystems, Carlsbad, California). The fluorescence threshold cycle value (Ct) was calculated by the instrument and the calculation of relative change in mRNA was made using the delta-delta method with correction for the housekeeping gene GAPDH and expressed relative to wild-type [62].

Table 2.1 List of primers

Human qRT-PCR primers		Primer Sequence (5' to 3')
Human GAPDH	Forward	GCAAATTCCATGGCACCGT
	Reverse	TCGCCCCACTTGATTTTGG
Human SASH1	Forward	TGCTGACTGGCCAGATGGTTCTTA
	Reverse	TCTGCGAGTGGAGTTTACCAGCTT
Mouse qRT-PCR primers		
Mouse GAPDH	Forward	TGAAGGTCGGTGTGAACGGATTTG
	Reverse	GGTCGTTGATGGCAACAATCTCCA
Mouse IL-6	Forward	ATCCAGTTGCCTTCTTGGGACTGA
	Reverse	TAAGCCTCCGACTTGTGAAGTGGT
Mouse IP-10	Forward	ATGAACCCAAGTGCTGCCGTCATT
	Reverse	TCAAGCTTCCCTATGGCCCTCATT

2.11 PCR

The PCR reaction was performed using 2 μL of DNA and 1.25 U of Taq DNA polymerase (New England Biolabs, Ipswich, MA). PCR for cloning the targeting construct was performed using Phusion High Fidelity polymerase (Finnzyme, Lafayette, CO) following manufacturer's instructions. PCR was performed on a PTC-200 PCR cycler (BioRad Laboratories, Hercules, CA). Samples were run on agarose gel. The gel was run in Tris-acetate EDTA buffer (TAE; 0.04 M Tris-acetate and 1 mM EDTA, pH 8.0). Primers are listed in Table 2.2.

Tabel 2.2 List of PCR primers

Genotyping Primers	Primer Sequence (5' to 3')	
LacZ	Forward	GCTGGATGCGGCGTGGGGT
	Reverse	CTGGATCAAATCTGTCGATCCTT
Sash1 WT allele	Forward	TCGAGAACTTCCATGCCCATCCTT
	Reverse	AGTCAGGTTGCCTATCTTGGCTGT
Open Reading Frame Primers		
A	Forward	AAGGGCCTCTAGCAAGGAGAGTAA
	Reverse	TCGGAAATTCTGCCAGAAGTAT
B	Forward	TGGAAAGGAAGGAGGGACAAACCA
	Reverse	TTGGTTCCAGGGACTGACTTGTGT
C	Forward	GGACATAAATAGCACTTGTGAGG
	Reverse	TTTCCTCCATCCTTCTGCCCGTAA
D	Forward	ATCTTAAGCGGACTTTTGGGCC
	Reverse	AAGCAGGTCGGAACTTTCTCAGTG
E	Forward	TTCCTTGGTGGTCTTTGCTTGTGC
	Reverse	AGATGGAGTATGGAACCTGCGTGA
F	Forward	TGCAGACTTCGCTTTACAGGCTGA
	Reverse	CTGCTGTGCCAGGTCATCAATGTT
G	Forward	CGGGTCCACAGGCGTCACTGTC
	Reverse	CTGCTGTGCCAGGTCATCAATGTT
Targeting construct clonging primers		
Homology arm I (HmI)	Forward	TTCTGCAGAGGGTAAAGCCTGAG
	Reverse	GCTCTAGAGATAAAAACCATGTCCTA
Floxed arm	Forward	TTGGATCCATTGATTTCTCTGTCCTT
	Reverse	TTGGATCCCATATGCGCGCTCACC
Homology arm II (HmII)	Forward	CTCGAGCATATGTGTGTGTGTG
	Reverse	GCAAGCTTCCATGGTAAGCAA
ESC sceening primers		
HmI upstream & *loxP*	Forward	CATATGGACCTGTCTGCTTCCTAGA
	Reverse	GATCCGGAACCCTTAATATAACTTC
LoxP & HmII downstream	Forward	CTTCGTATAGCATACATTATACGA
	Reverse	CTATCCATAAAGCAACACTCTGAGTC
Southern Blot probe primers		
SASH1 probe	Forward	AGGGCATTAGGGCAGTGAAGTTCT
	Reverse	ATCAGCCAGCTGCAATTTGATGGG
Selectable marker screening primers		
1 (Floxed arm and LoxP reverse)	Forward	TCCTCCCATCTCTTCTTACACAAC
	Reverse	GATCCGGAACCCTTAATATAACTTC
2F & 2Ra (HmI and Floxed arm)	Forward	CAGAAACTGCTTCTAAGTGTGTGT
	Reverse	AACTCTATAACAGCAGAGTTCG
2F & 2Rb (HmI and HmII)	Forward	CAGAAACTGCTTCTAAGTGTGTGT
	Reverse	CCAACTTAACCAAGGCTAATC

2.12 GENERATION OF SASH1 GENE-TRAP MICE

Gene-trapping is used to introduce insertional mutations across the genome in mouse embryonic stem cells (ESC). Gene-trap cassettes are inserted in a retroviral vector with the main elements being a promoterless reporter gene (β-geo) and a selectable marker flanked by an upstream splice acceptor sequence and a downstream polyadenylation sequence. Once inserted into an intron of a gene, the gene-trap cassette is transcribed from the endogenous promoter of that gene. Transcription is terminated at the inserted polyadenylation site in the gene trap cassette and the end product is a fusion protein encoding the truncated protein and the reporter marker. The insertion of the vector is mapped by 5' RACE and sequencing of the ESC clones. Thus, gene-trap concurrently mutates and reports expression of the endogenous gene.

SASH1-trapped ESC line CC0006 were obtained from the Sanger Institute Gene Trap Resource. Insertion of the gene-trap cassette into SASH1 locus was confirmed by RT-PCR using multiple forward primers and a reverse primer on β-geo and sequencing the PCR product. Clones of interest were then injected into the blastocysts of recipient females for development and birth at the Genetic Modeling Core of the BCCA. When pups were born, chimeric males containing cells derived from wild type and SASH1 gene-trap ESC were identified by having a mosaic coat color. Chimeras were then mated to wild type mice to identify SASH1 gene-trap mice by genotyping. Genomic DNA was isolated from mice by tail-digest with proteinase K followed by PCR using primers specific to the insertion site of the construct (see Table 2.2 for genotyping primers)

2.13 WHOLE MOUNT X-GAL STAIN

E 7.5, E8.5 and E9.5 embryos were dissected out and rinsed with PBS. Embryos were fixed in freshly prepared fixative solution of 1% paraformaldehyde (PFA), 0.2% glutaraldehyde

and 0.02% NF40 in PBS for 10 min at room temperature. Then embryos were rinsed with PBS-0.02% NP40 for 5 min three times followed by staining with freshly prepared β-galactosidase staining solution (10 μL of 40 mg/mL X-gal in 400 μL of solution A, which is composed of: 4 mM ferricyanide, 4 mM ferrocyanide, 1 M $MgCl_2$ in PBS) at 37^0C overnight. The following day embryos were rinsed with PBS-0.02%NP40-2 mM EDTA four times and placed in 50% glycerol followed by 80% glycerol at 4^0C.

2.14 X-GAL STAIN

P0 pups and E18.5 and E17.5 embryos were decapitated and the heads and bodies were prepared for sectioning separately. Whole lungs and embryos after dissection were fixed in 4% PFA at 4^0C overnight. Next day, they were washed three times with PBS and cryopreserved in 15% sucrose at 4^0C for 1 h, followed by incubation in 30% sucrose at 4^0C overnight. Tissues were placed into OCT compound and stored at 4^0C for 1 h to 3 h and then frozen at -80^0C until sectioning. 10 μm sections were cut and fixed with 0.2% glutaraldehyde staining solution (100 mM) sodium phosphate, pH 7.3, 2 mM $MgCl_2$, 0.01% sodium deoxycholate, 0.02% Nonidet-P40, 1 mg/mL X-gal, 5 mM ferrocyanide and 5 mM ferricyanide) at 37^0C overnight. Sections were counter-stained with nuclear fast red 1- 5 min and dehydrated with ethanol and xylenes according to standard protocols.

2.15 IMMUNOFLOURESCENCE STAINING

Sections were hydrated with PBS. A box was drawn around the tissue using ImmEdge pen and sections were fixed with 4% PFA for 5 min. Tissues were washed with PBS for 2 min and then blocked in blocking solution (5% Goat Serum, 0.2% TritonX and PBS) for 30 min. Tissues were incubated with Rat anti-Mouse CD31 (BD Pharmingen[TM] BD Biosciences, Mississauga, ON) in blocking solution at a concentration of 1:50 at 4^0C overnight. Tissues were

32

then washed in PBS and 0.2% TritonX three times and rinsed in PBS for 3 min. Secondary antibody (1:200, Alexa 594) in blocking solution was applied for 45 min. Tissues were washed in PBS and 0.2% TritonX three times and then rinsed in PBS for 3 min followed by counterstaining with DAPI (300 nM) for 1 min. Tissues were mounted in 50% Glycerol/PBS before analysis by immunofluorescent microscope.

2.16 EMBRYONIC STEM CELL (ESC) GENOMIC DNA EXTRACTION

Genomic DNA from ESC was isolated using DNAzol reagent following manufacturer's instructions (Invitrogen, Carlsbad, CA).

2.17 SOUTHERN BLOTTING

10 μg of genomic DNA from ESCs were digested with BglII and NcoI for 7- 8 h. Digested samples in loading buffer were loaded on 0.8% large agarose gel and electrophoresed at 30 V overnight. The next day, gel images were captured on Alpha Innotech Corporation gel doc and prepared for transfer by deurination in 0.1 M HCl for 8 min, denaturation in 0.5 M NaOH, 1.5 M NaCl for 30- 40 min, and rinsing with deionized water. DNA was transferred to Zetaprobe membranes (BioRad, Hercules, CA) by capillary transfer using 10X SSC buffer in the apparatus at room temperature overnight. The membrane was fixed at 80^0C for 1 hour in the sequencing gel dryer (Model 583, BioRad, Hercules, CA). The membranes were prehybridized in hybridization buffer (17 ml dH$_2$O, 0.2 g skim milk, 2 g dextran sulfate (Sigma-Aldrich, St. Louis, MO), 6 mL 20X SSC, 2 mL formamide (Invitrogen, Carlsbad, CA), 1 mL 20% SDS, 80 μL 500mM EDTA pH 8 and 1 mL 10 mg/mL Salmon sperm DNA (Sigma-Aldrich, St. Louis, MO) for 2 h at 65^0C. Denatured radioactive ^{32}P probe was added to each sample and probes were hybridized overnight at 65^0C in hybridization oven. Blots were washed with wash solution (0.3X

SSC, 0.1% SDS, 0.1% Tetra-Sodium Pyrophosphate) for 30 min for a total of 3 washes at 65^0C and then developed.

2.18 SEQUENCING

Sequencing was performed by Sanger Sequencing at the McGill university sequencing services (McGill university, QC), and samples were prepared as per established requirements. Table 2.3 shows the list of sequencing primers.

Table 2.3 List of sequencing primers

Targeting Construct	Primer Sequence (5' to 3')	
HmI	Forward	CATAGGTGGGCAGTCTCTGTCA
	Forward	CAGAAACTGCTTCTAAGTGTGTGT
	Forward	GGGCGACACGGAAATGTTGAATAC
	Forward	AAGTGCCACCTGACGTCTAAGA
	Reverse	CTGCGTGTTCGAATTCGCCAATGA
	Reverse	TAGCACTGTTCATCTTAGAGAC
	Reverse	AAGGTTCGTATCCTAGGCAGG
Floxed Arm	Forward	TGCCACTCCCACTGTCCTTTCCTAA
	Forward	GACAGAGCAGTGGTTTAGGGATGA
	Forward	GATGACCCCTGACCTTCACA
	Forward	TCCTCCATCTCTTCTTACACAAC
	Forward	GTAAGTCACTCTCCTCCCG
	Forward	AGGCTCATGAACCTGTTCTGT
	Reverse	AACTCTATAACAGCAGAGTTCG
	Reverse	GTATAGAGGGAGGACATGGCTG
	Reverse	CCTGGTAGATGTGCCACACAGAA
	Reverse	ATGGGAGTAGAGCTTACAGAGTC
HmII	Forward	GAAGAAGTGCTCTTCCTTCC
	Forward	AGCTCCGCTTCAGAACCAGCAA
	Forward	CAGGCTGGCCTCGAACTCAGAAA
	Reverse	ACTTACTCTCCAATAGCTCAG
	Reverse	CTGTAAAGCATGCACGTGCGC
	Reverse	GTGGTCCATCACAAGAATGTC
PCR cloning		
pDrive seq	Forward	TAATGCAGCTGGCACGACAGGTTT
	Reverse	CAGTCACGACGTTGTAAAACGACG

2.19 STATISTICAL ANALYSIS

Results are expressed as means +/- standard deviation (s.d). Error bars depict s.d. Chi-square test was performed using: http://www.graphpad.com/quickcalcs/chisquared1.cfm. P-values of less than 0.05 were considered significant.

CHAPTER 3: UNDERSTANDING THE ROLE OF SASH1 IN TLR4 SIGNALING AND CHARACTERIZATION OF SASH1 GENE-TRAP MICE

3.1 INTRODUCTION

Our lab has recently identified SASH1 as a novel regulator of the TLR4 signaling pathway. We have found that SASH1 binds to TRAF6 through its C-terminal TRAF domain using TRAF6 WT and SASH1 deletion mutants in reciprocal co-immunoprecipitation experiments (Dauphinee et al., manuscript submitted). Figure 3.1 depicts the structure of TRAF6. Endogenous interaction of SASH1 and TRAF6 is dependent on LPS stimulation. However, transient overexpression of SASH1 is sufficient to induce TRAF6 ubiquitination in HEK293-TLR4-MD2-CD14 cells. SASH1 also binds TAK1 and regulates its ubiquitination. We also confirmed that IKKβ and IKKα bind SASH1 using reciprocal coimmunoprecipitation experiments in HEK293T cells. However, SASH1 does not interact with MyD88, IRAK1, IRAK4, TRIF or TRAF3. The functional role of SASH1 in LPS signaling was measured through changes in activation of NF-κB and expression of proinflammatory cytokines upon LPS stimulation in shSASH1 HMEC (a human microvascular endothelial cell line). Knockdown of SASH1 in HMEC results in decreased NF-κB luciferase activity in response to LPS stimulation, but not in response to TLR2, TLR3, TLR5 and other signaling pathways that mediate signaling through TRAF6 such as TGFβR and IL-17R. SASH1 knockdown does not affect activation of an Interferon stimulated responsive element (ISRE) driving luciferase. LPS-stimulated SASH1 knockdown cells also produce decreased levels of proinflammatory cytokines IL-6 and IP-10. Thus, SASH1 acts as a scaffold protein that assembles a TRAF6/TAK1/ IKKβ complex downstream of TLR4 upon LPS stimulation (Dauphinee et al., manuscript submitted). Figure 3.2 shows a model for the role of SASH1 in endothelial TLR4 signaling.

Data in this chapter confirm the role of SASH1 as a positive regulator of TLR4 pathway in HMEC. We also show that SASH1 does not interact with Uev1A and Ubc13 and IKKγ. This

chapter also describes the generation of SASH1 homozygous gene-trap mice. Genotypic analysis of the heterozygous mouse crosses revealed no adult homozygous animals. Therefore, we hypothesized that SASH1 plays an important role in an earlier stage of mammalian development. To be able to study and understand the function of SASH1, different time points during development were examined and the presence of SASH1 homozygous gene-trap was found to cause perinatal lethality. Examining whole embryo sections of the homozygous gene-trap animals did not reveal any gross morphological defects in any organ except in the lungs where the airways appeared smaller than those of the wild-type lungs. SASH1 homozygous gene-trap animals may be dying due to lung defect. However, further investigation is required to define the cause of the perinatal death.

Figure 3.1 TRAF6 protein domains structure

TRAF6 has a RING domain that imparts E3 ligase activity, a Zn finger domain for ligase activity and a TRAF domain for binding to partner proteins. a.a, amino acids.
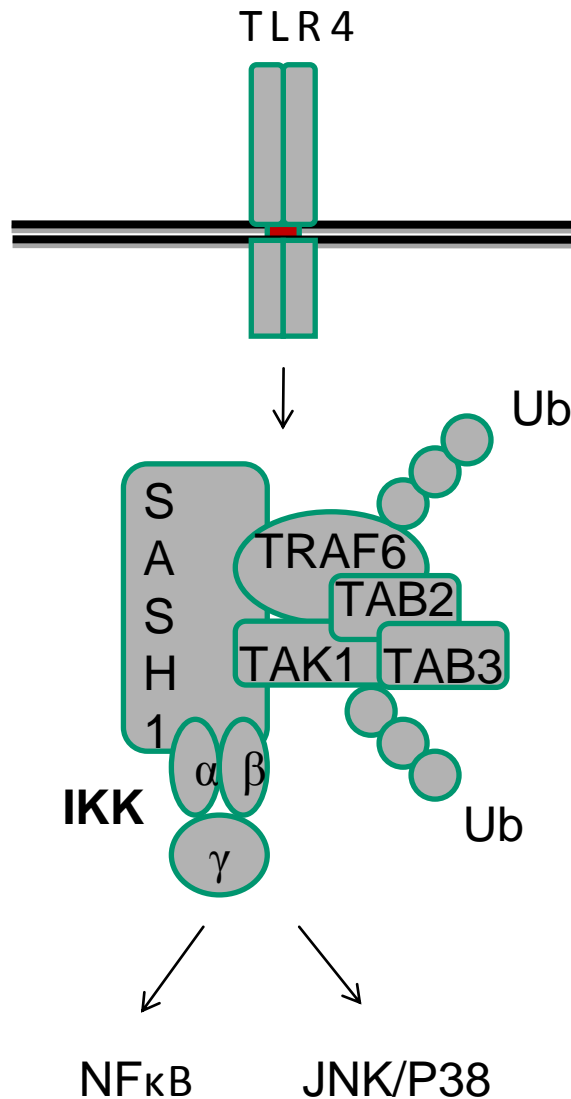
Figure 3.2 A model for the role of SASH1 in endothelial TLR4 signaling

SASH1 is a scaffold protein that binds to TRAF6/TAK1/IKKβ/IKKα and promotes TRAF6 ubiquitination, resulting in activation of NF-κB and JNK, and culminating in the increased production of proinflammatory cytokines. TLR4 activation by LPS is required for the activation of downstream signaling and production of proinflammatory cytokines. TLR4, Toll-like receptor 4; MyD88, myeloid differentiation factor 8; TRIF, Toll/interleukin-1 receptor-containing adaptor inducing interferon β; SASH1, SAM and SH3 domain-containing protein; TRAF6, tumor necrosis factor receptor-associated factor 6; TAK1, transforming growth factor β-activated kinase 1; IKK, IκB kinase; NF-κB, nuclear transcription factor-κB; Ub, ubiquitin; LPS, Lipopolysaccharide.

3.2 RESULTS

3.2.1 SASH1 knockdown and NF-κB activation

Previously in our lab, a lentiviral-delivered shRNA targeting SASH1 was used to infect HMEC. SASH1 knockdown resulted in decreased NF-κB luciferase activity and reduced IL-6 production from LPS stimulated HMEC (data not shown, Dauphinee et al., manuscript submitted). Here I confirm this result using a different knockdown construct. As expected, SASH1 knockdown resulted in a significant decrease in NF-κB luciferase activity in LPS stimulated HMEC (Figure 3.3).

As an alternative approach to the luciferase reporter assay, I also compared IκB degradation levels in SASH1 knockdown (shSASH1) HMEC after LPS stimulation. The IκB complex keeps NF-κB in the cytoplasm under normal conditions. Upon stimulation, IKK phosphorylates the IκB complex resulting in its degradation and release of NF-κB that translocates to nucleus. Thus, decreased IκBα degradation is an indication of decreased NF-κB activation. HMEC transduced with SASH1 knockdown vector (F1) or empty vector control PLKO.1 were analyzed for IκBα degradation by Western Blot after 0, 15, 30, 60, 90 and 120 min of LPS stimulation. Decreased degradation of IκBα was detected in SASH1 knockdown cells as opposed to vector control starting at 30 min LPS stimulation (Figure 3.4).
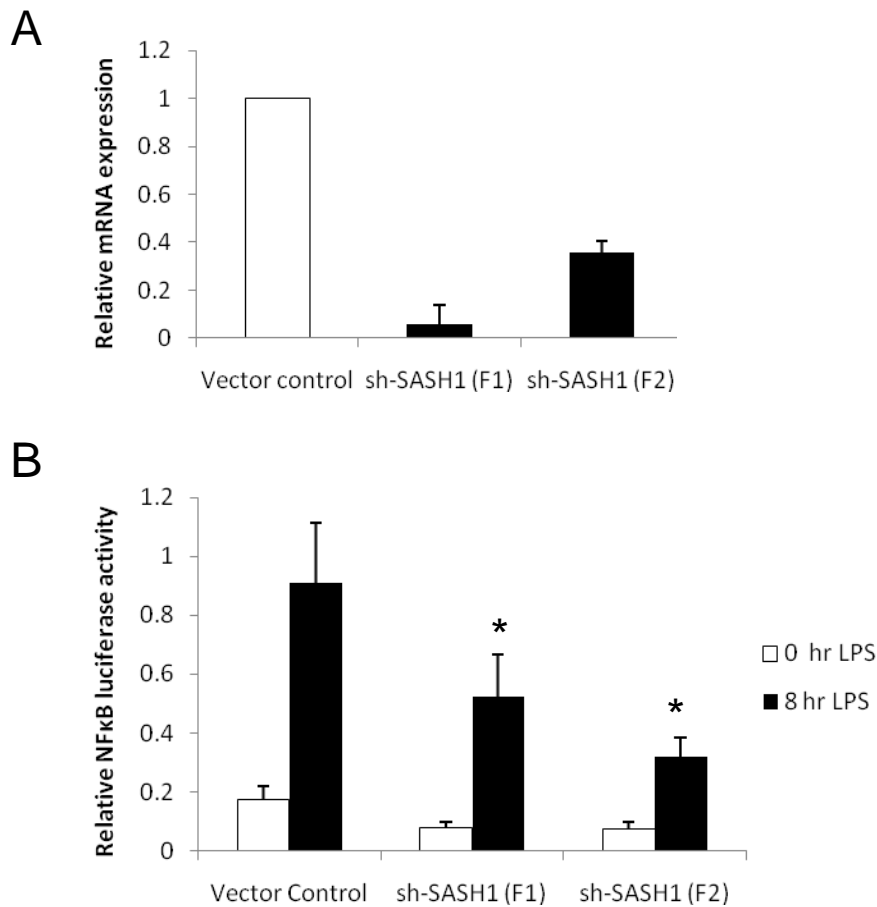
Figure 3.3 SASH1 knockdown decreases LPS signaling

HMEC were transduced with lentiviral vector encoding shRNA targeting SASH1 or PLKO.1 vector control. SASH1 knockdown was confirmed by RT-qPCR (A). HMEC were transduced with pNF-κB-Luc plus pRL-CMV for measurement of luciferase reporter activity after LPS stimulation (100 ng/mL, 8 hr). *P = 0.05 is determined by Student's *t-test*. Error bars indicate standard deviation. The luciferase assay graph (B) was plotted using data compiled from three independent experiments with each experiment containing triplicates for each parameter.
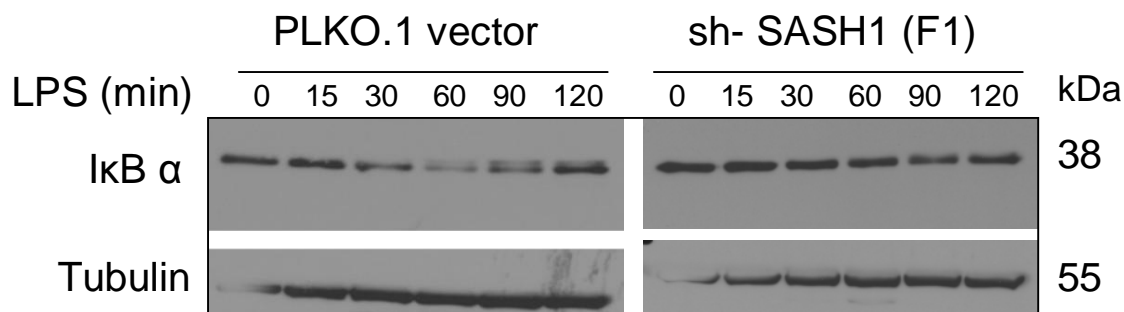
Figure 3.4 SASH1 knockdown HMEC show decreased IκBα degradation compared to vector control

HMEC were transduced with lentiviral vector encoding shRNA targeting SASH1 or PLKO.1 empty vector control. SASH1 knockdown was confirmed by RT-qPCR. HMEC transduced with shSASH1 or PLKO.1 vector control were then treated with LPS (100 ng/mL) at indicated timepoints. Activation of NF-κB was analyzed by probing for IκBα and tubulin was used as a loading control. This experiment was performed with only one shRNA SASH1 contruct.

3.2.2 Investigation of SASH1 interaction with Uev1A and Ubc13

TRAF6 ubiquitination is required for the formation of a downstream signaling complex of TAK1 and the adaptor proteins TAB2 and TAB3. Shauna Dauphinee in our lab discovered

that transient overexpression of SASH1 in HEK293-TLR4-CD14-MD2 cells was sufficient to induce auto-ubiquitination of TRAF6 in the absence of LPS stimulation (Dauphinee et al., manuscript submitted).

TRAF6 ubiquitination requires interaction with E2 conjugating enzymes (Ubc13 and Uev1A) [41] to catalyze the linkage of Lysine-63 (K63)-linked polyubiquitin chains on itself. TRAF6 binds directly to Ubc13, but not Uev1A [63]. We did not detect an interaction between SASH1 and either Ubc13 or Uev1A (Figure 3.5A and B, respectively). However, we were able to detect interaction between TRAF6 and Ubc13 as well as between Ubc13 and Uev1A (Figure 3.5C and D). These results suggest that SASH1 does not directly bind the E2 ligases, but that the E2 ligases are incorportated into a complex by binding TRAF6 and each other. It remains unclear though how SASH1 induces TRAF6 ubiquitination in the absence of stimulation and it is possible that a secondary signal through LPS-TLR4 is required to complete the activation of the signaling a cascade.
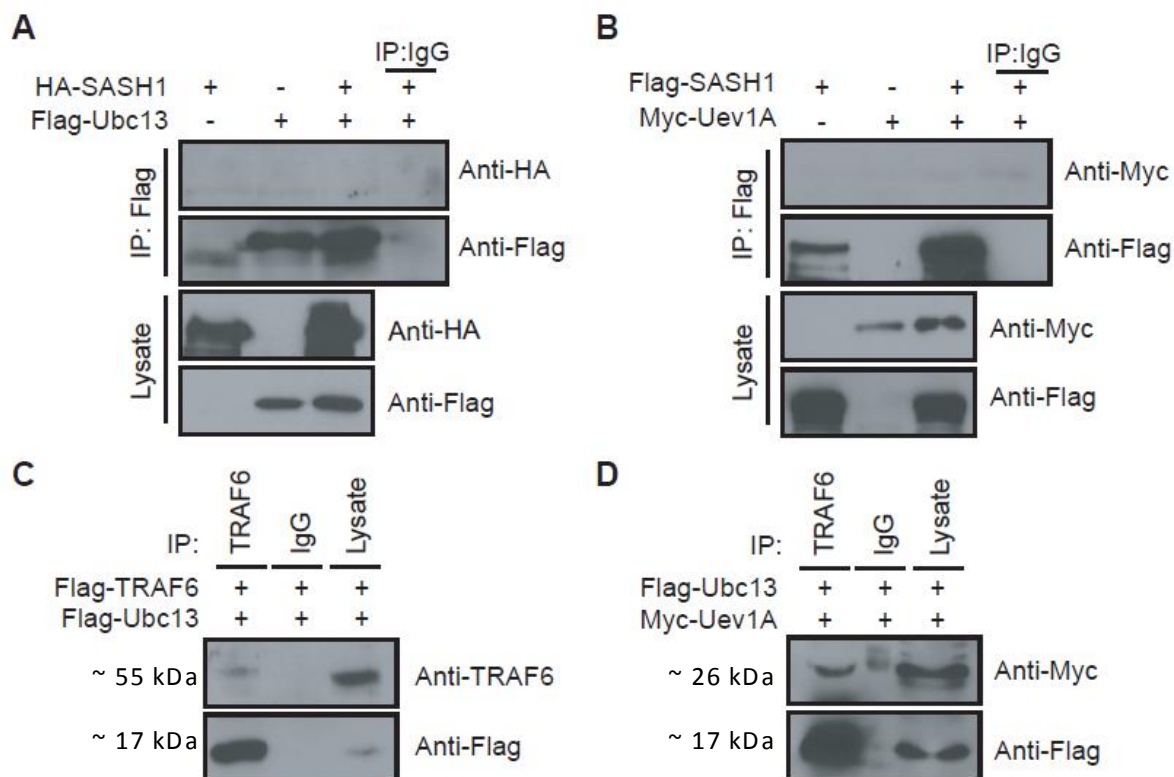
Figure 3.5 SASH1 does not interact with Ubc13 and Uev1A.

HEK293T cells were co-transfected with (**A**) HA-SASH1 and Flag-Ubc13, (**B**) Flag-SASH1 and Myc-Uev1A, (**C**) Flag-TRAF6 and Flag-Ubc13 or (**D**) Flag-Ubc13 and Myc-Uev1A and lysates were immunoprecipitated (IP) and immunoblotted with antibodies to HA, Flag and Myc. Panel **C** was performed by Shauna Dauphinee once. Panel **A** was performed by both Shauna Dauphinee and me a total of 4 times. I performed panel **B** and **D** thrice and once, respectively. Molecular weights: SASH1, 170 kDa; Ubc13, 17 kDa; Uev1A, 26 kDa; TRAF6, 55 kDa.

3.2.2 Investigation of SASH1 interaction with IKKγ

As already mentioned, reciprocal coimmunoprecipitation experiments in our lab demonstrated that SASH1 interacts with TRAF6, TAK1, IKKβ and IKKα (Dauphinee et al., manuscript submitted).. IKKβ is part of a complex consisting of an additional catalytic subunit, IKKα, and a regulatory subunit, IKKγ. Reciprocal coimmunoprecipitation revealed that SASH1

45

does not interact with IKKγ although we were able to detect interaction between IKKγ and IKKβ as a control (Figure 3.6A and B, respectively). Thus, while SASH1 can directly bind to IKKα and IKKβ, it does not directly interact with IKKγ.
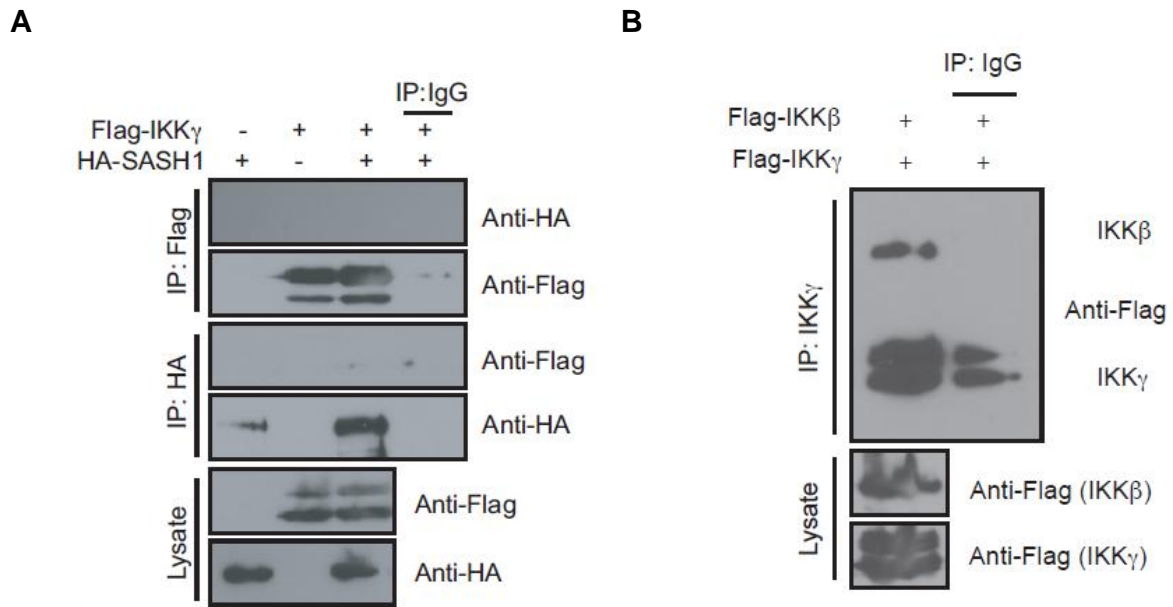
Figure 3.6 SASH1 does not interact with IKKγ

A. SASH1 does not interact with IKKγ. HEK-293T cells were co-transfected with HA-SASH1 and Flag IKKγ and lysates were IPed and immunoblotted with antibodies to HA and Flag. **B**. IKKγ interacts with IKKβ. HEK 293T cells were co-transfected with Flag-IKKγ and IKKβ and Iped for IKKγ and immunoblotted with anti-Flag. Panel **A** was performed by both Shauna Dauphinee and me for a total of 4 times. Panel **B** was performed once by me. Molecular weights: IKKγ, 48 kDa; SASH1, 170 kDa; IKKβ, 87 kDa.

3.2.4 Generation of SASH1 gene-trap mouse

To examine the *in vivo* function of SASH1 in TLR4 signaling, our lab generated SASH1 homozygous gene-trap mice that resulted in a SASH1-LacZ fusion protein under control of the endogenous promoter of SASH1. The SASH1-LacZ fusion disrupts the SASH1 gene at intron 14 truncating the SH3 domain and resulting in loss of the two SAM domains and TRAF6 binding domain (Figure 3.7). Genotypic analysis of the heterozygote crosses did not reveal any viable SASH1 homozygous gene-trap mice from a total of 55 pups examined ($p<0.0005$, chi square test). However, the heterozygous gene-trap mice were grossly normal and fertile (Dauphinee et al., manuscript submitted).

In order to measure the expression level of SASH1, we performed RT-qPCR on tissues harvested from wild type adult mice (Figure 3.8). There is higher expression of SASH1 in spleen, heart and lung. However, SASH1 is expressed in all the tissues examined. SASH1 has been reported to have ubiquitous expression in human tissues [57].

Since gene-trap mice have the β-geo cassette inserted into SASH1 locus, we investigated SASH1 *in vivo* expression pattern in adult heterozygous tissues by X-gal staining. The result showed that SASH1 is highly expressed in microvascular endothelium of spleen, lung and thymus (Figure 3.9A, B, and C). SASH1 was also found in the parenchyma of the liver, kidney and brain (Dauphinee et al., manuscript submitted).
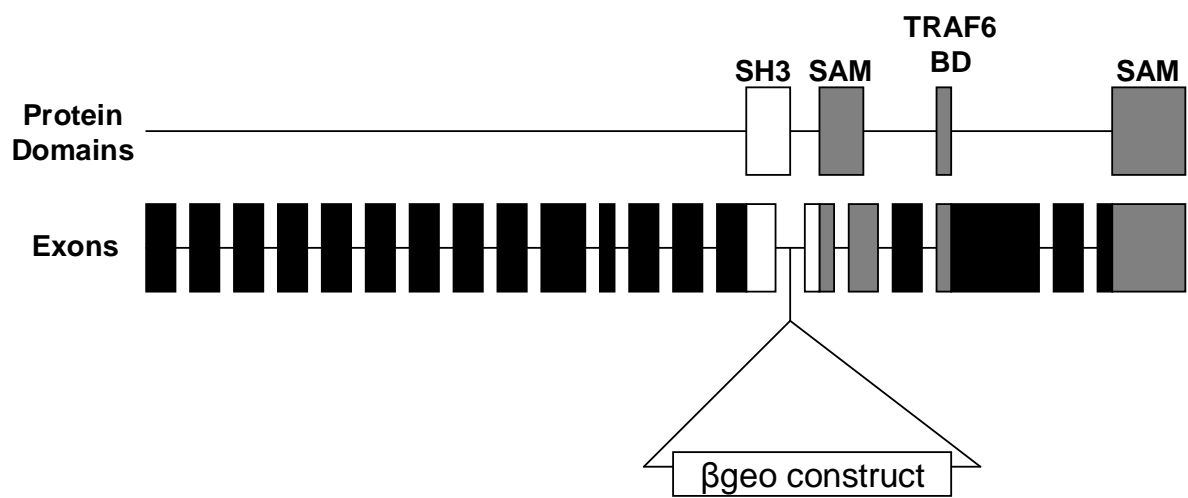
Figure 3.7 Generation of gene-trap SASH1 mice

Gene-trap mice were generated from ES cells by a senior graduate student, Shauna Dauphinee. (A) The genomic insertion was mapped to intron 14-15 using PCR and Southern Blot. SASH1 gene-trap did not produce viable adult homozygous mice (P<0.0005, chi square test) (Dauphinee et al., manuscript submitted).

qPCR-murine tissues relative to Spleen
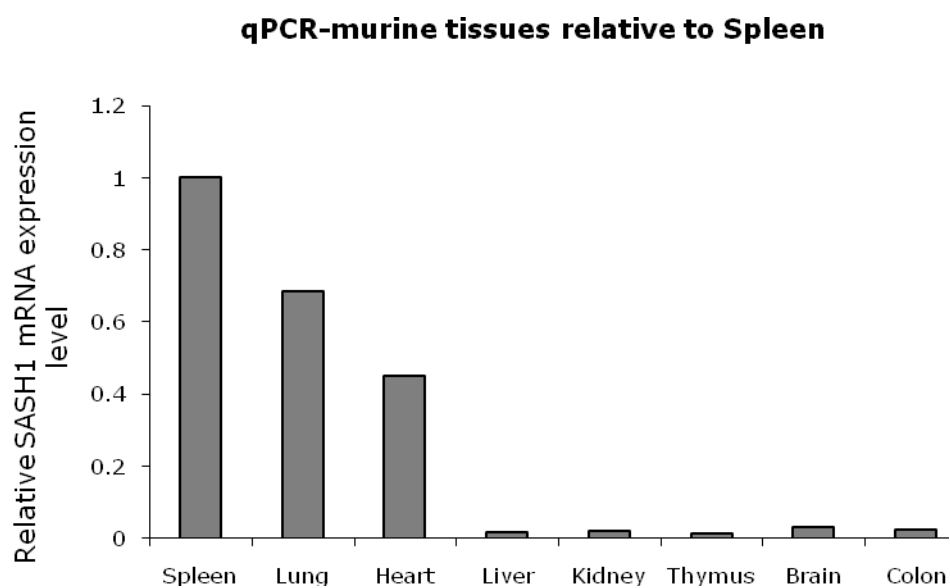
Figure 3.8 SASH1 mRNA is expressed in mouse tissues

qPCR was performed on RNA isolated from tissues harvested from C57BL/6 mice using qPCR primers specific to mSASH1. GAPDH was used as an internal control. SASH1 mRNA expression is high in spleen, lung and heart. However, it is expressed in all tissues examined..
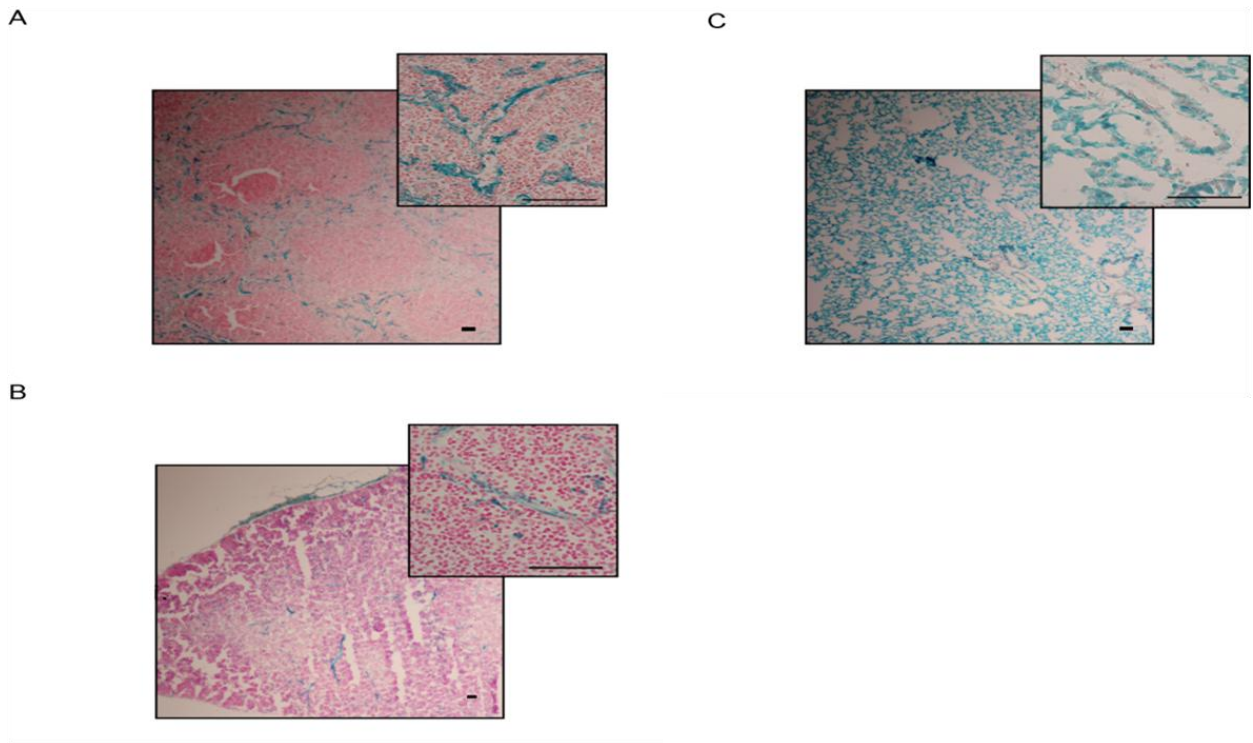
Figure 3.9 SASH1 is primarily expressed in the endothelium of spleen, thymus and lung.

X-gal staining shows SASH1 expression primarily in endothelium of (**A**) spleen, (**B**) thymus, (**C**) lung in heterozygous adult mice tissues. However, SASH1 is also expressed in the parenchyma of liver, kidney and brain. X-gal staining was performed by me twice.

3.3.5 Investigation of SASH1 homozygous gene-trap lethality time point during development

In order to characterize the cause of death in SASH1 homozygous gene-trap, we aimed to define the exact stage of lethality by in-depth genotypic analysis and X-gal staining of various stages during development. Figure 3.10 shows our genotyping strategy using two sets of primers (A) and an example of the genotyping result (B). Considering SASH1 is primarily expressed in endothelium in adult heterozygous tissues and the fact that endothelial cells originate around E8.0, we first looked at E7.5 and E8.5 followed by E9.5. Figure 3.11 shows results of the whole-mount X-gal staining at E7.5 (A), E8.5 (B) and E9.5 (C). SASH1 homozygous gene-trap embryos were found at all the above stages examined. However, the homozygous gene-trap embryos did not show any gross morphological defect or delay in their development compared to the wild-type and heterozygous embryos. This also shows that SASH1 promoter is active during development. SASH1 homozygous gene-trap embryos were also present at E13.5 and E17.5. We then followed the heterozygous genetic crosses further and allowed the litters to give birth to examine the newborn pups. No live homozygous gene-trap animals were discovered at birth with a significant chi-square P-value of 0.0171 (Figure 3.12A). This indicates that homozygosity for the *Sash1* gene-trap allele results in perinatal lethality. Furthermore, within the same experiment genotypic analysis of the 6 pups that were discovered dead revealed that they were all homozygous for *Sash1* gene-trap allele. This data fits a Mendelian ratio of 1:2:1 (p=0.6, chi square) (Figure 3.12B).

A. Two primer sets were designed: one on *LacZ* gene and the other on an intronic region spanning the β-geo construct. **B**. Agarose gel image where sample 3, 4, 5 and 7 are WT, 1, 6 and 9 are heterozygous and 2 and 8 are SASH1 homozygous gene-trap.
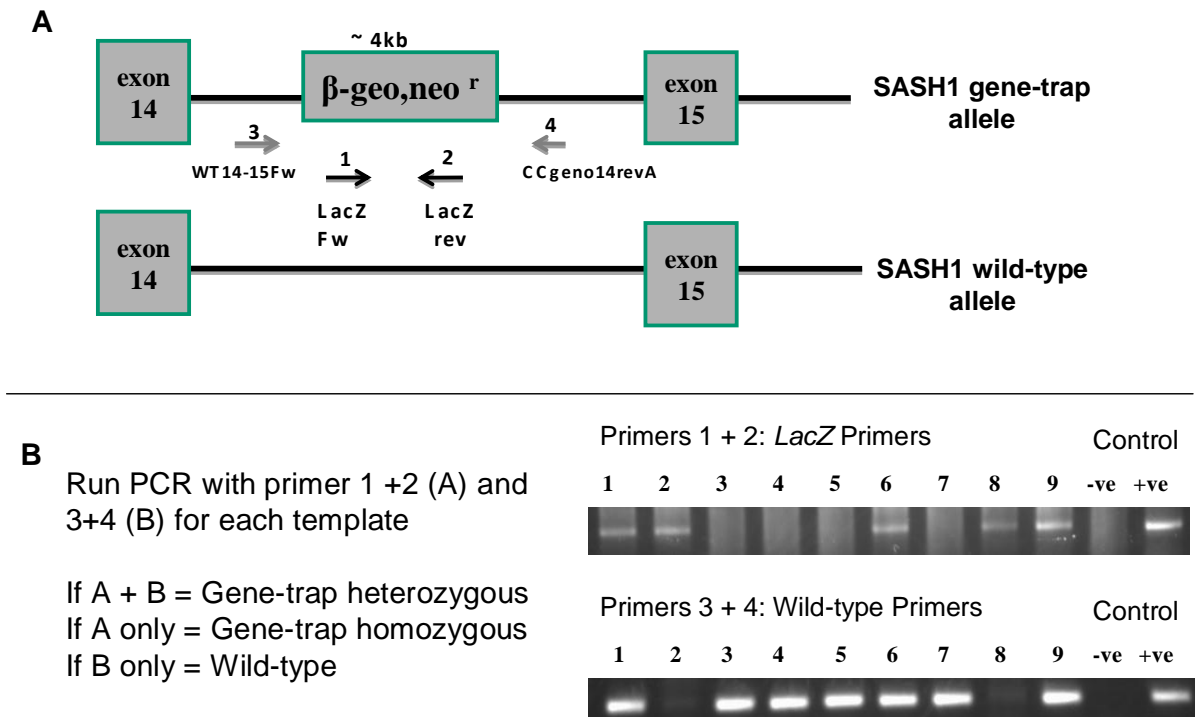
Figure 3.10 SASH1 gene-trap mice genotyping strategy

	Wild-type	Gene-trap heterozygous	Gene-trap homozygous	
A				E7.5
B				E8.5
C				E9.5
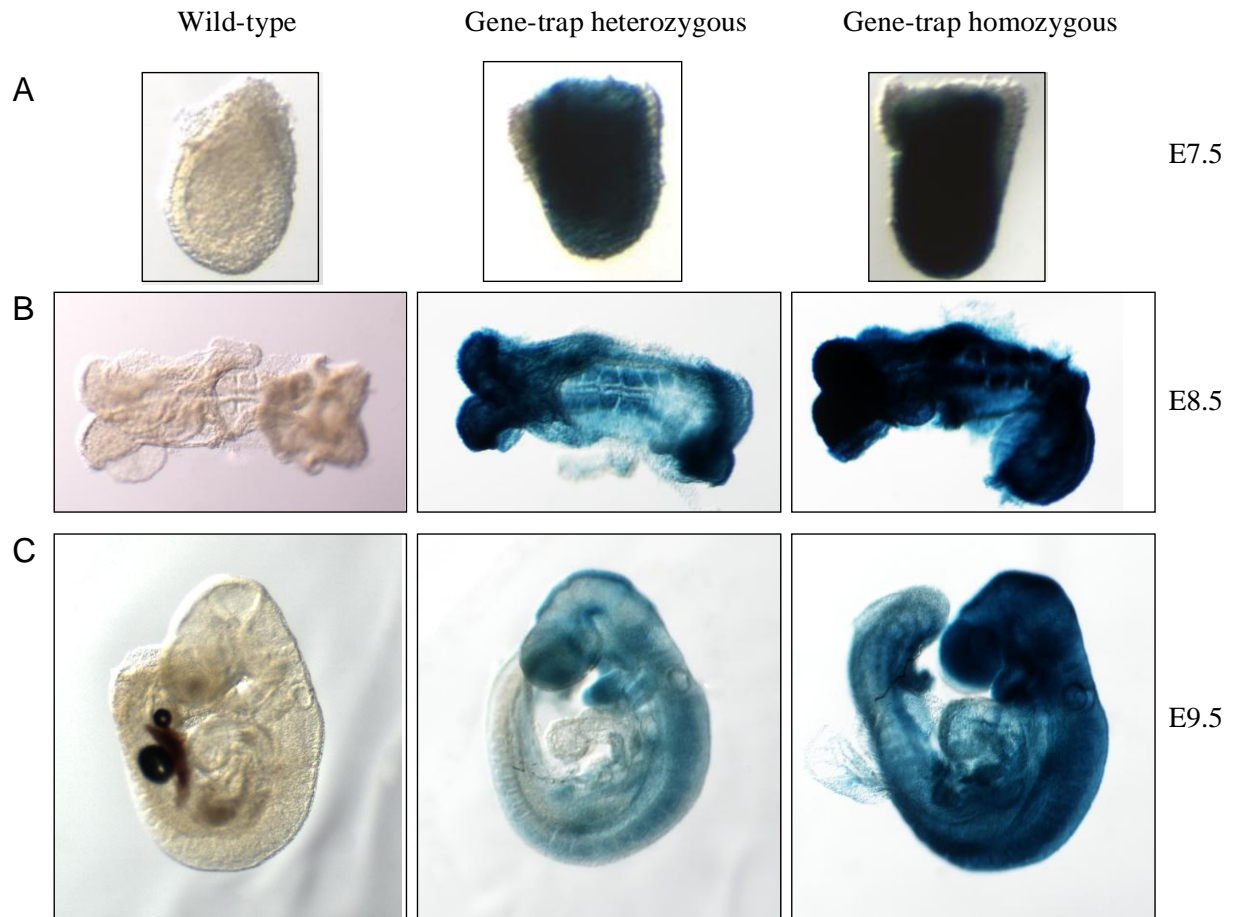
Figure 3.11 SASH1 homozygous gene-trap embryos do not show any gross morphological difference compared to WT and heterozygous embryos at E7.5, E8.5 and E9.5

Embryos were dissected from pregnant heterozygous females at E7.5 (**A**), E8.5 (**B**) and E9.5 (**C**). Yolk sack from each embryo was isolated for genotyping and the whole mount X-gal stain was performed. There is no gross morphological difference or developmental delay in the SASH1 homozygous gene-trap embryos compared to wild-type and heterozygotes at E7.5 (A), E8.5 (B) and E9.5 (C). This experiment was performed once. However, more than one embryo of each genotype was examined at each time point.

A

Genotype	Observed live pups after birth	Expected live pups after birth	Chi-squared p-value
Wild-type	5	5.25	0.0171
Gene-trap heterozygous	16	10.5	
Gene-trap homozygous	0	5.25	
total	21		

B

Genotype	Observed	Expected	Chi-squared p-value
Wild-type	5	6.75	0.6
Gene-trap heterozygous	16	13.5	
Gene-trap homozygous	6	6.75	
Total	27		

Figure 3.12 SASH1 homozygous gene-trap pups die perinatally

SASH1$^{+/-}$ crosses were set up and pregnant females' cages were monitored immediately after birth. Pups from each litter were collected right after birth. Tails were collected for genotyping. **A.** Of the 21 pups analyzed, no live homozygous gene-trap was found. This results in a significant p-value of 0.0171. Thus, homozygosity for the *Sash1* gene-trap allele results in perinatal death. **B**. From a total of 27 pups born, 6 were found dead and identified as homozygous gene-trap based on genotypic analysis. Since our observed result of 6 dead pups is not significantly different than the expected ratio, our result fits the Mendelian ratio of 1:2:1.

3.3.6 Investigation of the cause of SASH1 homozygous gene-trap perinatal death

In order to start investigating the cause of death, we performed H&E staining using E17.5 embryos. We did not detect obvious difference in organs such as the liver, heart and brain (Figure 3.13). However, lungs from homozygous gene-trap pups had smaller airways compared to those of wild-type and heterozygous gene-traps (Figure 3.14). We then performed X-gal staining on P0 lungs and it also showed that the lungs of SASH1 homozygous gene-trap have smaller airways compared to wild-type and heterozygous lungs (Figure 3.15)

Since SASH1 is primarily expressed in the endothelium of the lung in the adult heterozygous gene-trap mice, we performed immunofluorescent staining against the endothelial cell marker, CD31, to examine the overall morphology and pattern of endothelial cells in SASH1 homozygous gene-trap lungs. As seen in figure 3.15, we found that the airways in SASH1 homozygous gene-trap lungs appear mis-shaped. This brings up the possibility of the epithelial cells of the airway being affected possibly due to an imbalance in endothelial and epithelial coordination during development. It is possible that disruption of SASH1 impairs the ability of endothelial cells to act as regulator and supporter of epithelial cells during development. Normal lung morphogenesis and development depend on interactive signaling between epithelial cells and the surrounding mesenchymal cells [14, 16]. Endothelial cells have been shown to be essential for airways development and maturation [14, 16]. SASH1 might play an essential TLR4 independent function in the lung development. However, this is a preliminary result and needs to be validated and studied further. It is also possible that during embryogenesis, SASH1 is expressed in epithelium or both endothelium and epithelium.
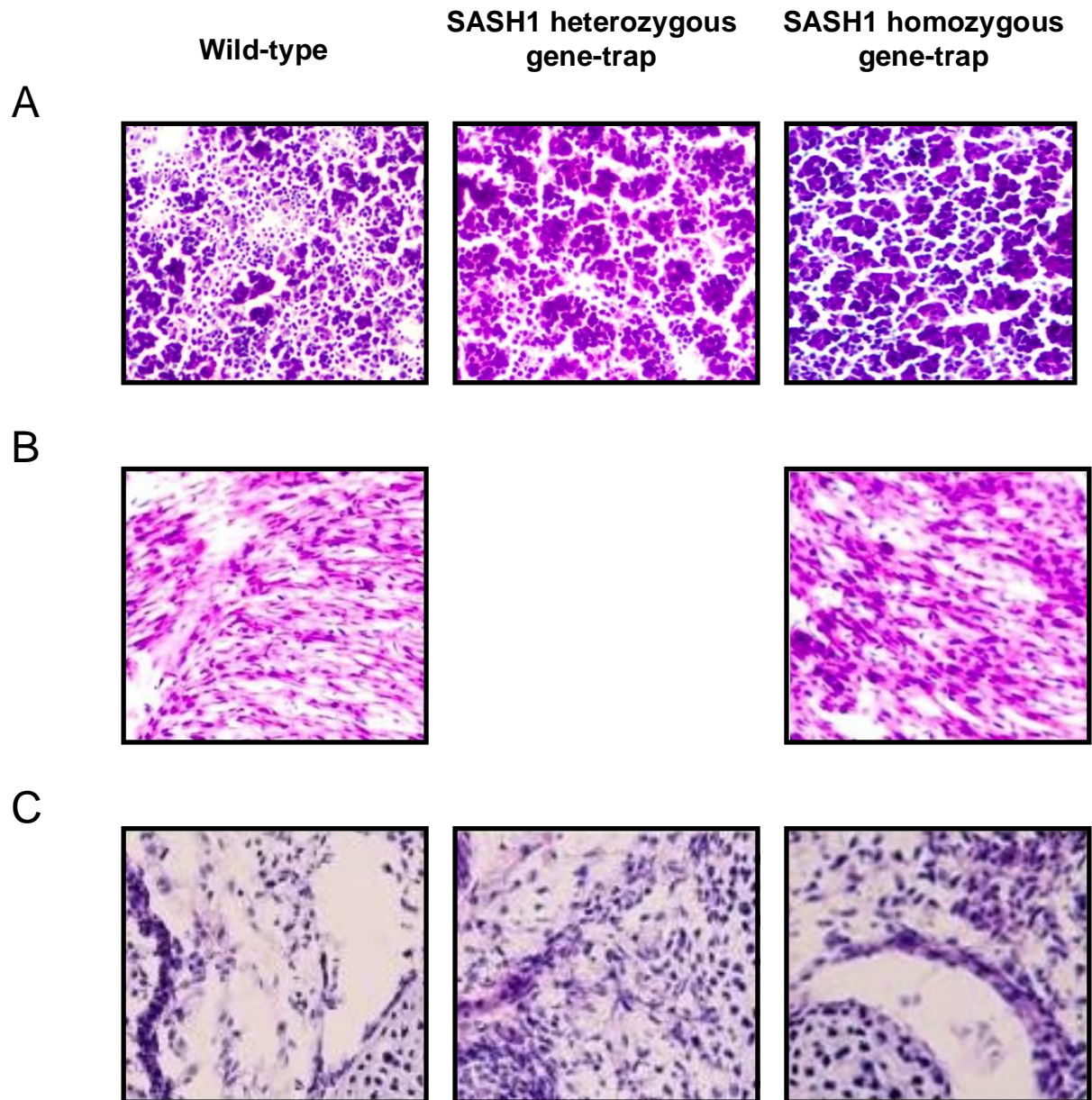
Figure 3.13 H&E stain of SASH1 homozygous gene-trap liver, heart and brain

E17.5 embryos were taken out of the mother by C-section. Tails were collected for genotyping after embryos were decapitated. **A, B** and **C** are H&E stain of the liver, heart and brain, respectively**.** We do not have the H&E stain for heterozygous gene-trap heart. There is no obvious difference in the liver, heart and brain of SASH1 homozygous gene-trap compared to those of wild-type.

Wild-type   Gene-trap heterozygous   Gene-trap homozygous

A

B
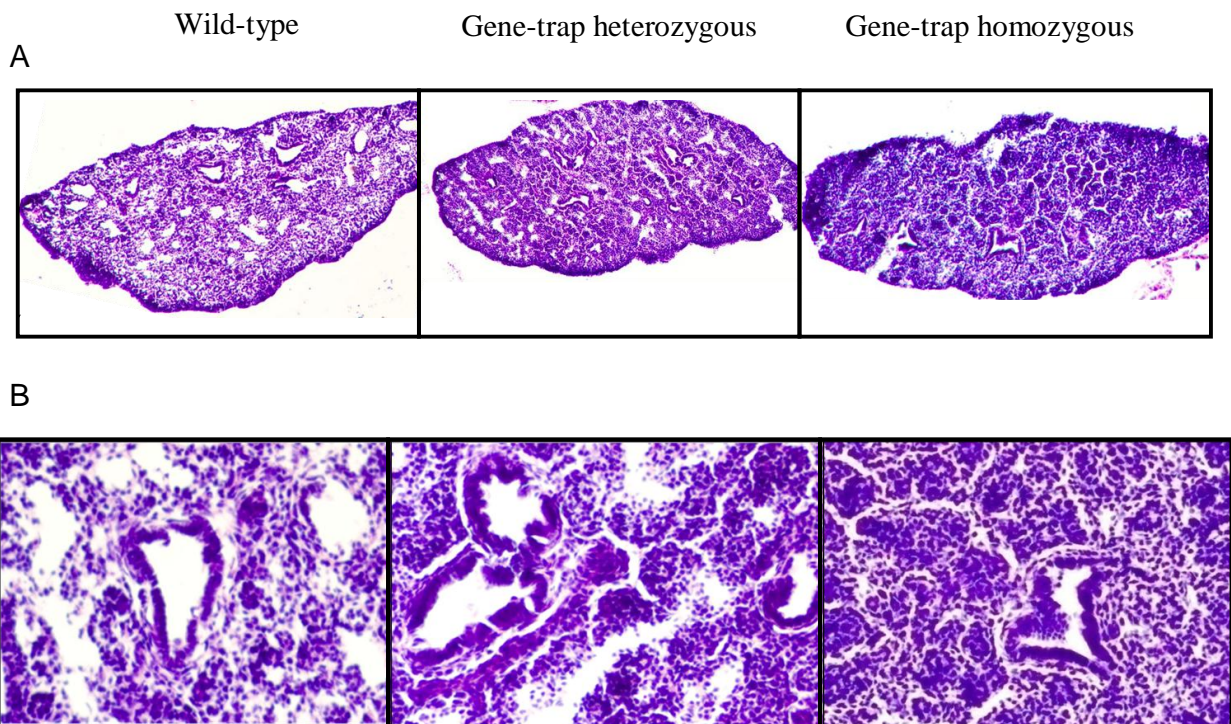
Figure 3.14 SASH1 homozygous gene-trap lungs have smaller airways at E17.5

E17.5 embryos were taken out of the mother by C-section. Tails were collected for genotyping after embryos were decapitated. **A and B.** H&E stain of the lungs viewed at 4X and 20 X magnifications. Airways in the SASH1 homozygous gene-trap lungs appear smaller than those in the heterozygous and wild-type lungs. H&E staining was performed on two different animals.

Wild-type

Gene-trap heterozygous

Gene-trap homozygous
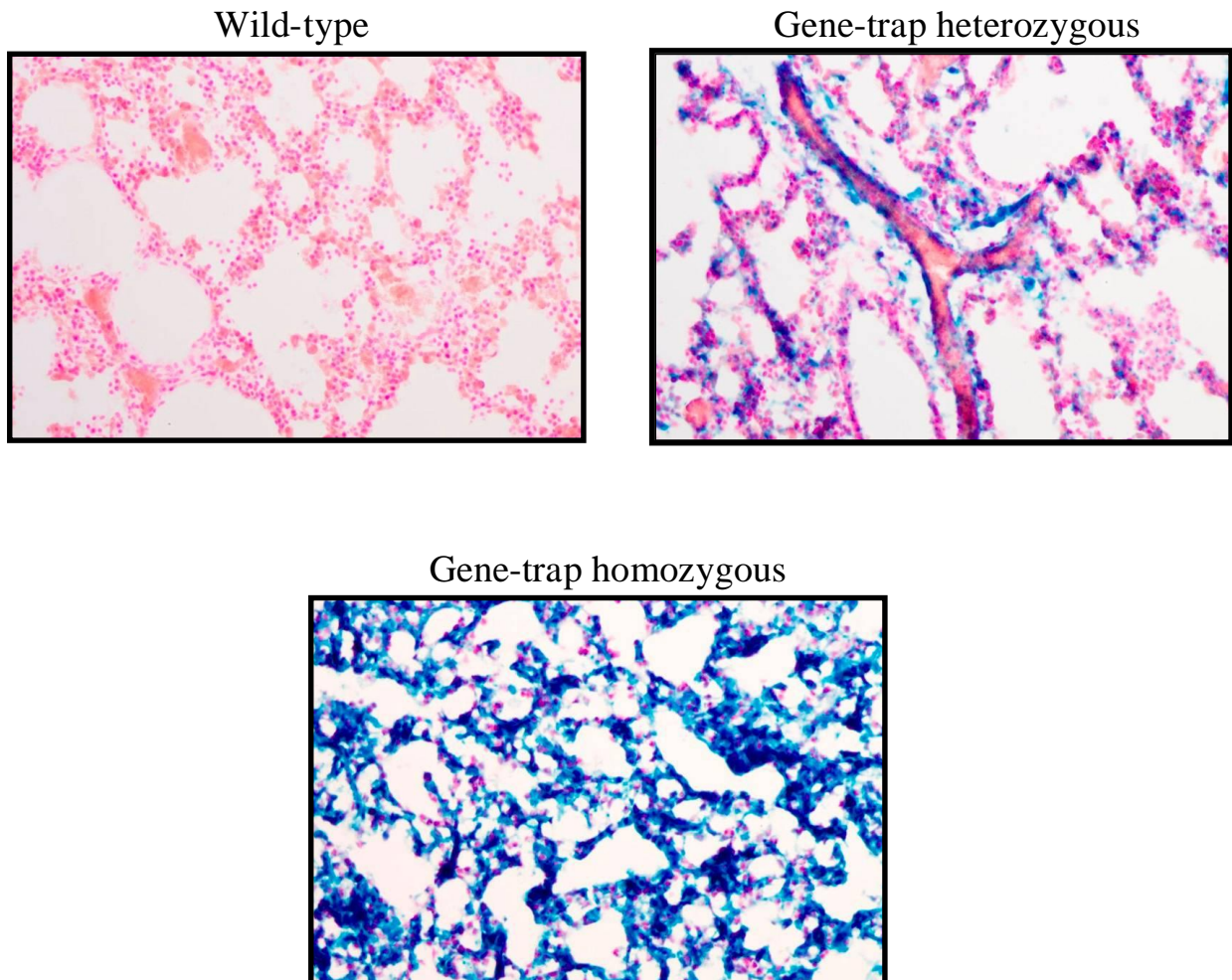
Figure 3.15 SASH1 homozygous gene-trap lungs have smaller airways at P0

X-gal and nuclear fast red staining of P0 lungs viewed with 20x magnification. Pups were collected shortly after they were born at P0. Tails were collected for genotyping and lungs were dissected out, fixed and OCT embedded before staining. Airways in SASH1 homozygous gene-trap lungs are smaller than those in heterozygous and wild-type lungs. X-gal staining was performed on three different animals.
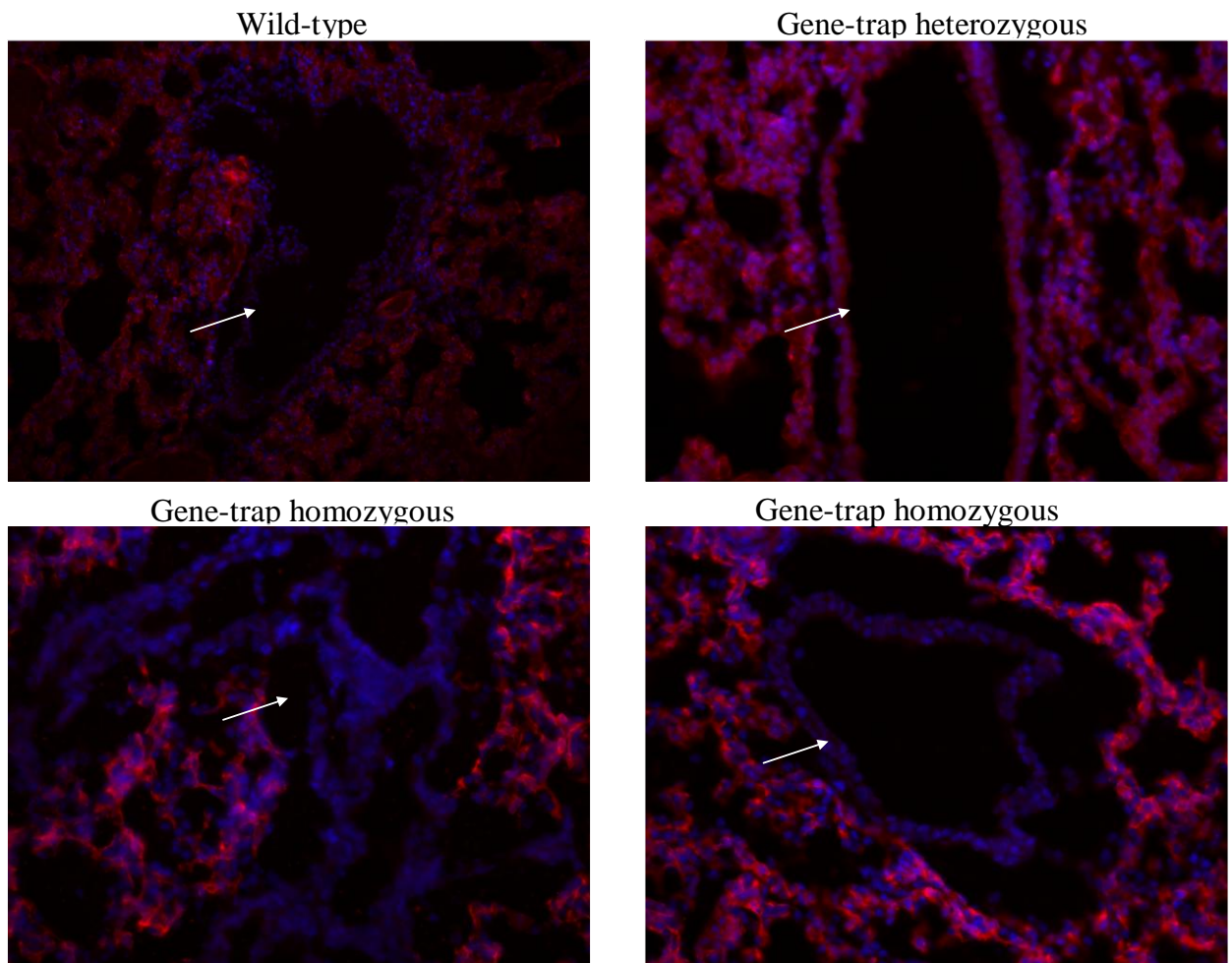
Figure 3.16 SASH1 homozygous gene-trap lungs have smaller and in some cases mis-shaped airways

Immunofluorescent staining against CD31, an endothelial cell marker, was performed on frozen lung sections. Nuclei were stained with DAPI (blue). Red color marks endothelial cells, while blue marks nuclei. Airways do not contain any endothelial cells. Airways are indicated with white arrows. This experiment was performed on two different animals.

3.3.7 Examination of SASH1 homozygous gene-trap lungs

In addition to microscopic examination, we also examined the gross morphology of the whole lungs at P0 and E18.5. SASH1 homozygous gene-trap pups die 15-20 min after birth or after they are delivered, while the live pups were terminated by decapitation before their lungs were dissected out and examined. We found that SASH1 homozygous gene-trap lungs were not inflated, while wild-type and heterozygous lungs were inflated (Figure 3.17). One way to verify lung inflation is to submerge a lung in PBS and observe whether it sinks or floats [64]. We examined P0 and E18.5 lungs and found that the wild-type and SASH1 heterozygous gene-trap lungs floated, while all lungs from SASH1 homozygous gene-trap mice sank to the bottom (Figure 3.18A, B and C). One wild-type lung at P0 sank to the bottom. This was most likely due to a puncture accidently introduced into the lung during the dissection procedure. This experiment along with the microscopic observation of the lungs show that homozygous deficiencies for SASH1 results in a failure of lung inflation. Lack of inflation could be due to a developmental defect or surfactant deficiency in the lungs or lack of respiration caused by a primary defect somewhere else. Thus, the following questions still need to be answered: is SASH1 homozygous gene-trap lung defect the primary cause of lethality; and is the deflated lung phenotype and difference in airway appearance a secondary effect of death due to respiratory failure?

Wild-type

Gene-trap heterozygous

Gene-trap homozygous

Gene-trap homozygous
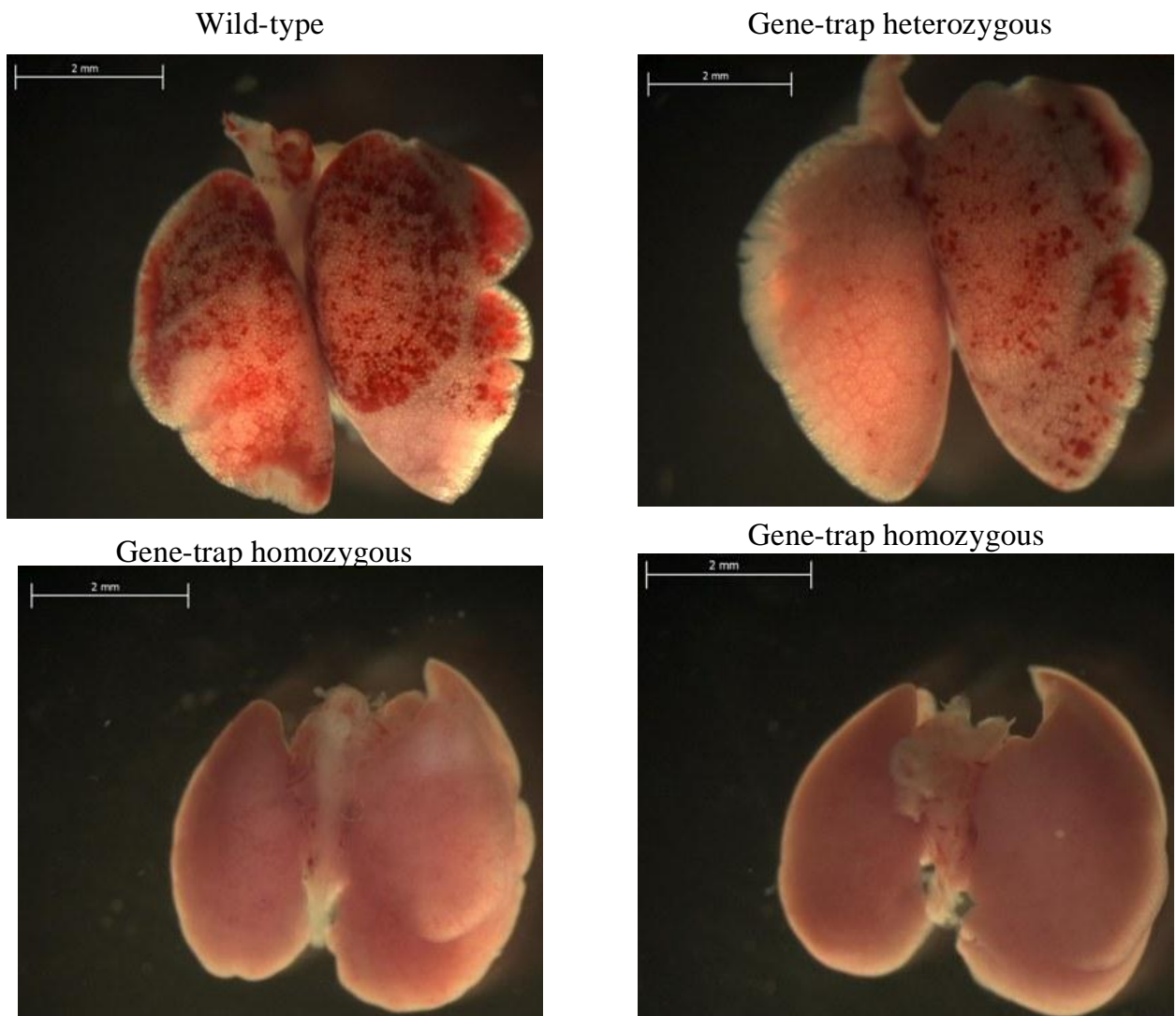
Figure 3.17 SASH1 homozygous gene-trap lungs appear deflated compared to wild-type and heterozygous lungs

Pups were either taken out of the pregnant mother at E18.5 by C-section or were collected after they were born at P0. SASH1 homozygous gene-trap pups die ~15 minutes after birth or being outside the mother. Homozygous gene-trap lungs looked deflated. 27 lungs from E18.5 pups and 32 lungs from P0 pups from six different litters at each time point were examined for their gross morphology.
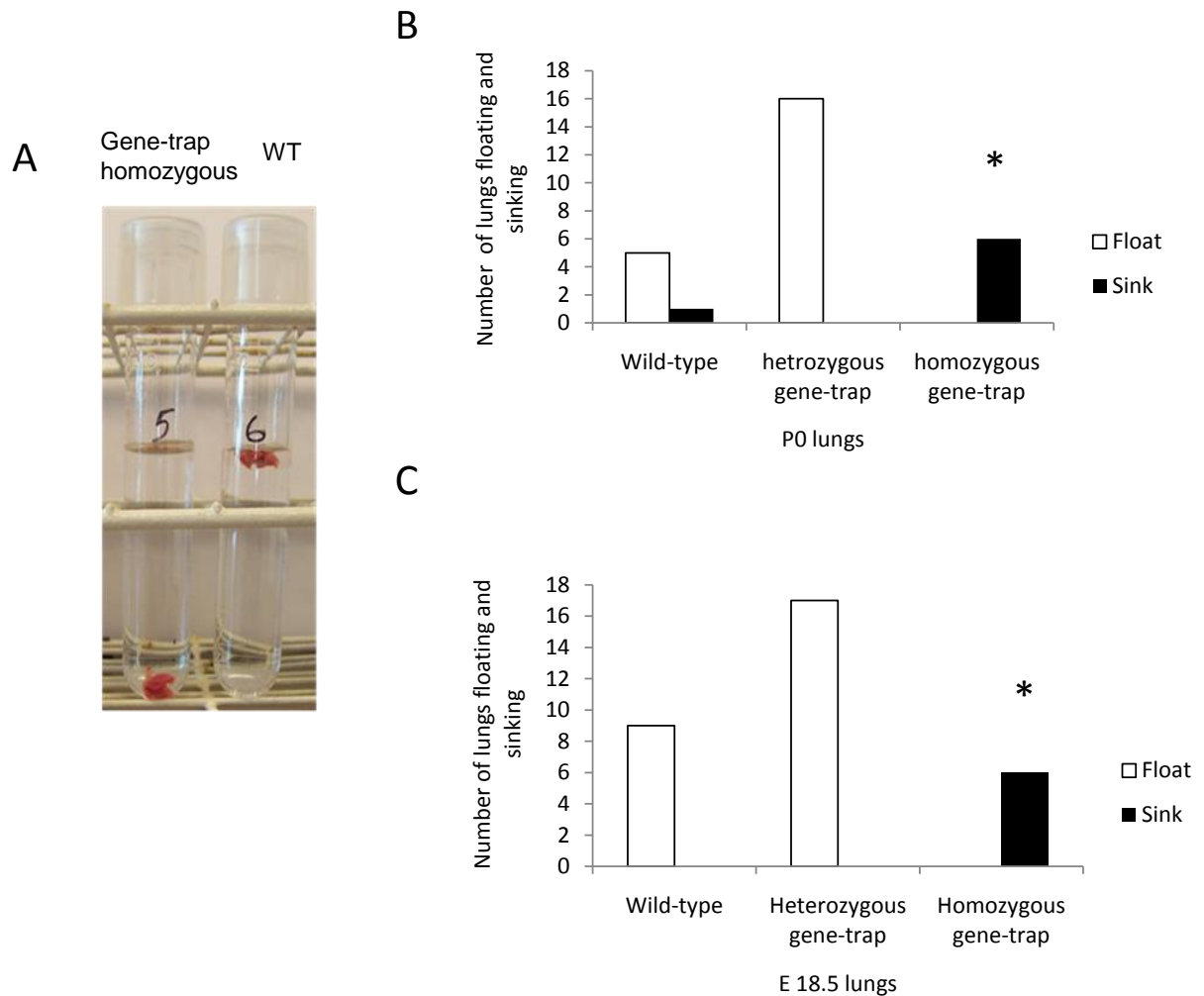
Figure 3.18 SASH1 homozygous gene-trap lungs sink in PBS

A. Pups were taken out of the pregnant mother at E18.5 by c-section or were collected after they were born at P0. SASH1 homozygous gene-trap lungs sink to the bottom while wild type and heterozygous lungs float on the surface. This indicates that homozygous gene-trap lungs are not inflated. **B and C.** data showing the number of lungs examined at P0 and E18.5, respectively. *P-value of <0.0001 was determined by Fisher's exact test using contingency analysis for both P0 and E18.5 lungs.

3.3 DISCUSSION

The data presented in this chapter confirms the role of SASH1 in activation of NF-κB in the TLR4 pathway. We also found that homozygosity for the *Sash1* gene-trap allele results in perinatal death and the lungs of SASH1 homozygous gene-trap animals appear deflated and sink in PBS. In addition, airways of SASH1 homozygous gene-trap lungs appear smaller than those of wild-type and heterozygous lungs by X-gal and immunofluorescence staining. However, morphometric analysis of the lungs should be performed to conclusively claim whether there is any defect in the lung. This issue is discussed in detail in chapter 5.

It still remains unclear whether the pups die due to a defect in the lungs or somewhere else. A thorough investigation of all the organs in addition to the lungs should be performed to characterize SASH1 homozygous gene-trap mice. Thus, this chapter provides the basis for further studies in understanding the *in vivo* role of SASH1 during development.

Since homozygosity for the *Sash1* gene-trap allele results in perinatal death, we attempted to isolate and immortalize SASH1 gene-trap endothelial cells to test the activity of NFκB and expression of proinflammatory cytokines. We attempted to isolate endothelial cells by staining for endothelial marker, CD31, and sorting the positive cells from embryos at E9.5, E 13.5 and E 16.5. However, despite multiple troubleshooting endeavors, we were unable to grow and immortalize the isolated endothelial cells in culture. Alternatively, we attempted to obtain MEFs from SASH1 homozygous gene-trap embryos. MEFs from SASH1 homozygous gene-trap did not have any gross morphological difference compared to wild type cells. However, we were not able to obtain enough RNA to test expression of proinflammatory cytokines by qPCR. Thus, it will be interesting to test NFκB activity and expression of proinflamamtory cytokines in future.

CHAPTER 4. GENERATION OF SASH1-FLOXED EMBRYONIC STEM CELLS

4.1 INTRODUCTION

SASH1 is a scaffold protein that assembles TRAF6/TAK1/IKKβ/IKKα downstream of TLR4 upon LPS stimulation. SASH1 functional response to LPS was shown by increased production of proinflammatory cytokines in SASH1-overexpressing HMEC upon stimulation (Dauphinee et al., manuscript submitted). SASH1 is primarily expressed in endothelial cells of spleen, thymus and lung as well as in parenchymal cells of liver, kidney and brain. SASH1 homozygous gene-trap results in perinatal death.

Since SASH1 plays a critical role in endothelial TLR4 signaling and SASH1 homozygous gene-trap results in perinatal death, endothelial specific deletion of SASH1 in adult mice will be important in understanding the *in vivo* function of SASH1 in response to LPS and in LPS-induced sepsis. It will also allow us to understand the role of SASH1 in the endothelium. Thus, we aimed to generate SASH1-floxed embryonic stem cells (ESC) that could be used to generate conditional SASH-null mice. Based on previous studies, one can hypothesize that the response of endothelial targeted SASH1^{-/-} mice to LPS will be similar to that seen in MyD88^{-/-} mice [65] and that the endothelial-specific deletion of SASH1 will reduce the inflammatory effects of endotoxemia.

We chose the *Cre/lox* system to delete SASH1 specifically in endothelial cells [66]. To use this system, we would need to generate SASH1[flox/flox] mice and an endothelial specific Cre driver mouse such as VE-Cadherin-Cre (VEC) line. Our lab has already generated a VEC-Cre strain, which drives endothelial cell-specific expression of Cre recombinase (unpublished data). Our lab has shown specific EC expression of this line by crossing with Rosa-flox-stop-lacZ mice. Cre is a recombinase from P1 bacteriophage [66]. The Cre catalyzes site-specific recombination by crossover between two Cre recognition sequences called a *loxp* site that is 34

bp in length. DNA sequences introduced between two the *loxP* sites get excised in a head to tail orientation during Cre-mediated recombination [66]. Cre expression can be controlled both spatially by using a tissue-specific promoter and temporally by using an inducible system [66].

The data presented in this chapter show generation of ESC with a targeted allele of *Sash1* with the help of the Genetic Modeling Core of the BCCA. We designed our targeting strategy by selecting a suitable region of the gene void of other putative Open-Reading-Frames (ORF) and miRNA. We chose to flox exon 3 and 4 to generate a stop codon in exon 5 when the floxed region is excised. ESCs were then electroporated with the cloned targeting construct and screened by PCR. Southern blot analysis was used to confirm two positive clones. The presence of *loxP* sites in positive clones was also confirmed by sequencing. Once the selectable marker is successfully removed, these floxed-ESCs can be used to generate SASH-floxed mice, allowing us to study the role of SASH1 *in vivo*.

4.2 RESULTS

4.2.1 SASH1 targeting strategy to generate SASH1 floxed-ESC and mice

Since SASH1 is a large gene of 20 exons and huge introns, it is not possible to flox the whole gene. We selected to flox exon 3 and 4 to generate an out-of-frame mutation resulting in a stop codon in exon 5 when the floxed region is excised. This will result in a loss of the remainder of the gene. The targeting strategy is shown in figure 4.1.
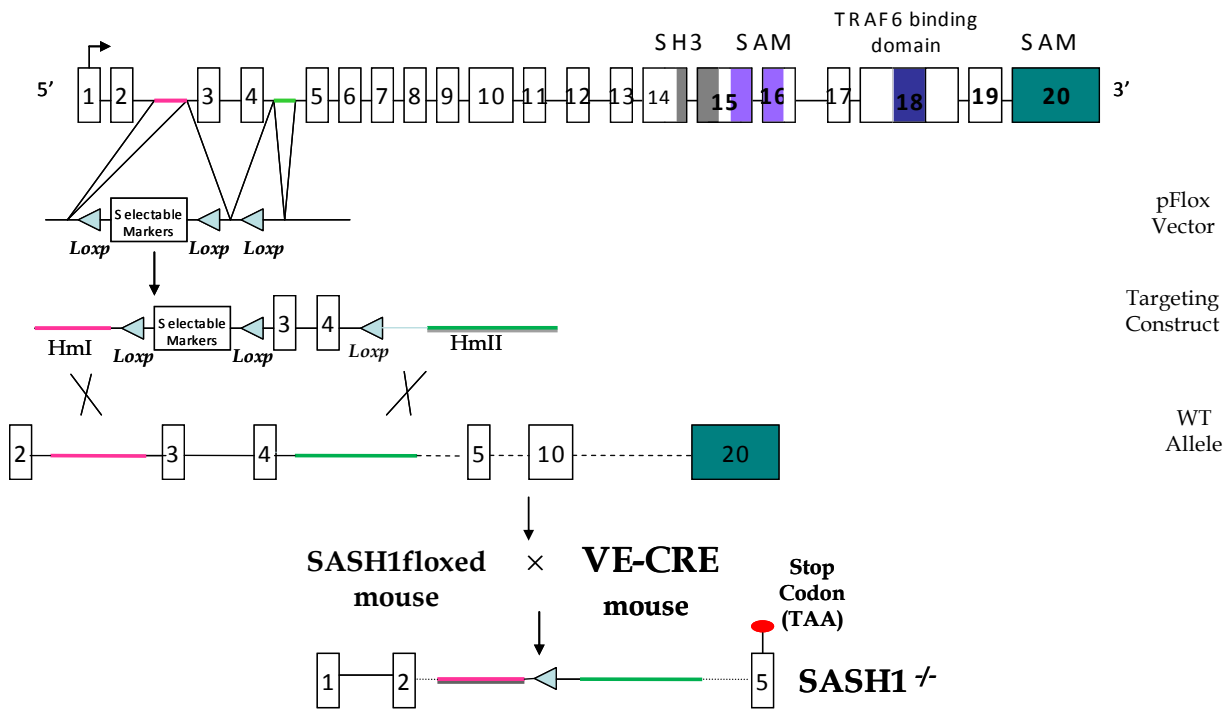
Figure 4.1 Murine SASH1 locus and targeting strategy

The top part of the figure outlines murine SASH1 exons highlighting the protein domains. Below is the targeting strategy. Exon 3 and 4 were selected to be floxed as their excision with Cre recombinase would generate a stop codon in exon 5. Exon 3 and 4 were cloned in between the two *loxP* sites and the intronic regions upstream and downstream were cloned as homology arm I (HmI) and homology arm II (HmII), respectively. The targeting construct was then electroporated into ESC for homologous recombination to occur. ESCs were screened for positive clones and confirmed by Southern blotting and sequencing.

Once positive clones are identified, the selectable marker will be removed and the ESC will be injected into blastocysts which are transferred to the uterus of a recipient mouse acting as a surrogate mother. 8-week old chimeras, pups containing tissues from the modified brown ESCs and the black recipient, will be bred with black coat females. Brown offspring from the cross will be tested for the genetic modification and positive mice will be bred together to create SASH1$^{flox/+}$ mice. The flox line will then be backcrossed to C57Bl/6J. SASH1 $^{flox/+}$ on C57Bl/6J will be crossed together to create SASH1$^{flox/flox}$ mice. The floxed line will then be crossed to the VEC-Cre line to delete SASH1 specifically in the endothelial cells.

4.2.2 Investigation of the presence of Open Reading Frames (ORFs) in the region to be floxed

Four bacterial artificial chromosomes (BAC) on the 129 background, containing the SASH1 gene, were obtained (Centre for Applied Genomics, Toronto). We designed primers and sequenced all four of the BACs and found one of them to be of interest to us that contained the 5' UTR to exon 8 of SASH1. To make sure we did not disrupt any other overlapping gene by our targeting strategy, we searched for the presence of coding and non-coding genes including microRNAs. No other genes or miRNA were found to overlap SASH1 using UCSC genome browser and miRBase. UCSC genome browser predicted overlapping ORFs in the region of interest (Figure 4.2A). To confirm the presence of these ORFs, RT-PCR was performed using primers specific to ORF's exons overlapping SASH1 introns. RT-PCR did not amplify any bands indicating the ORFs were not expressed in wild-type murine tissues (Figure 4.2B).
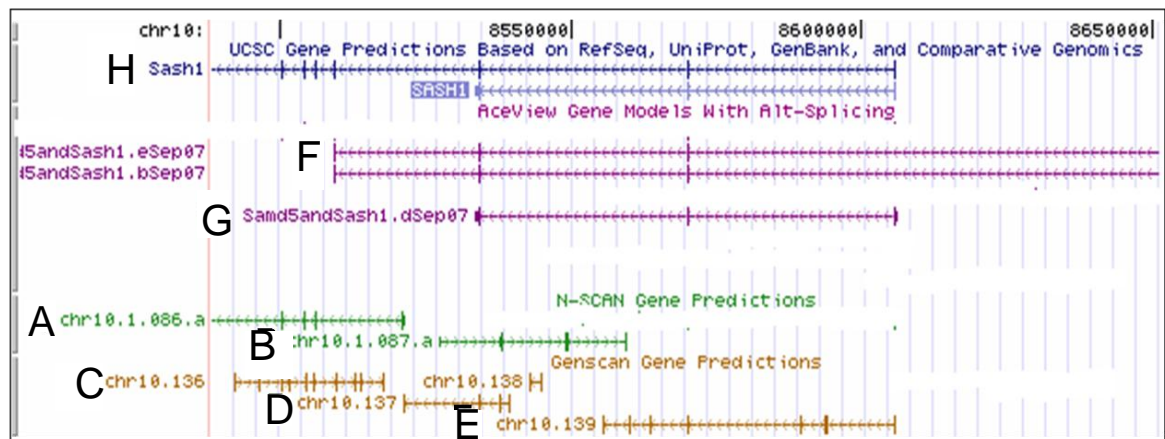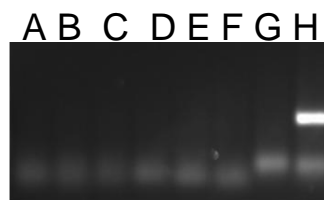
Figure 4.2 RT-PCR did not amplify the UCSC predicted ORFs overlapping the exon 3 and 4 of SASH1 and the genomic region around it

A. Snapshot of UCSC showing predicted ORF overlapping SASH1 exon 3 and 4 genomic region. **B.** Wild-type murine tissues were harvested and total RNA was isolated for CDNA synthesis. RT-PCR was performed using primers specific to predicted ORFs' exons overlapping SASH1 introns. None of the predicted ORFs were amplified (lane A-G) and while primers against SASH1 gave correct size of band as a control (lane H). This experiment was performed once.

4.2.3 Cloning of SASH1 exon 3 and 4 and homology arm I and homology arm II into the pFlox vector

Exon 3 and 4, homology arm I (HmI) and homology arm II (HmII) were PCR amplified from 129 genomic BAC using primers designed to contain appropriate 5' restriction sites with high fidelity Phusion Taq Polymerase. PCR products were then cloned into pFlox sequentially to create the targeting construct, which was then sequenced. The targeting construct was aligned with the reference sequence and analyzed for the introduction of any mutations during its cloning. The targeting construct was linearized and electroporated into ESC. Figure 4.3 shows the targeting construct along with PCR screening strategy.

4.2.4 Homologous Recombination screening strategy and result

ESC were screened by PCR and confirmed through Southern blot. The PCR screening strategy is shown in figure 4.3. 384 ESC clones were screened for the presence of the 1st *loxP* site using primers against sequences upstream of HmI and *loxP* site (Primer set 1, Figure 4.3A). Four positive clones were identified in the first PCR screen (Figure 4.3B). I then performed Southern blot to confirm our result. Figure 4.4 shows the Southern Blot screening strategy and result. Of the four clones, two were found to be true positives (Figure 4.4). Presence of the third *loxP* site with HmII was confirmed in the two positive clones through PCR and sequencing (Figure 4.5). Before removing the selectable marker, the presence of the second *loxP* site was also confirmed by PCR and sequencing. The result is shown in figure 4.6. Thus, we have generated *Sash1* floxed ESCs that is required for making conditional targeted *Sash1* mice.

A
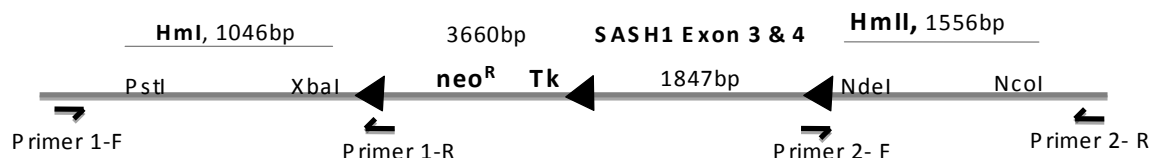
B
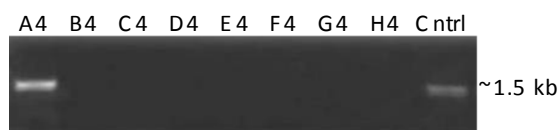
Figure 4.3 PCR screening strategy and results

A Schematic of the targeting construct along with the PCR screening strategy shown by primer set 1 and primer set 2. Tk: Thymidine Kinase. **B.** ESCs, electroporated with targeting construct, were grown on neomycin and the resistant clones were replicated and lysed. Genomic DNA was isolated and PCR using primer set-1 was performed. Of the 384 clones screened for first *loxP* site, 4 positives were found. We had also cloned a positive control containing only HmI to be used as control. P1-A4 (lane1) was one of the positives found shown here as an example.
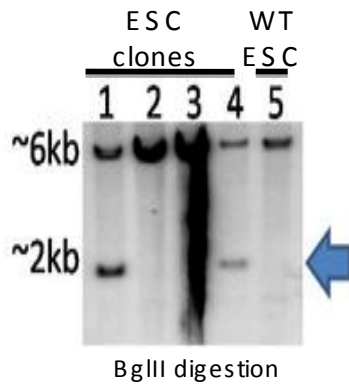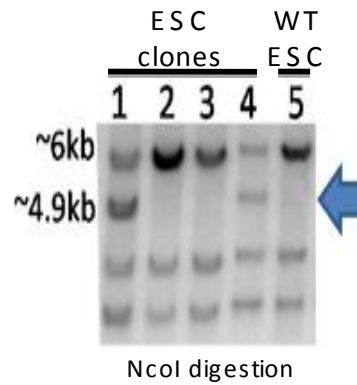
Figure 4.4 Southern blot screening strategy and results

A. Southern blot screening strategy using BglII restriction enzyme for genomic digestion. A second BglII site is introduced upon homologous recombination of the targeting construct. **B and C.** Showing Southern blot result with BglII and NcoI digestion, respectively. Of the four positives found through PCR, two of the clones (1-P1A4 and 4-P4D3) were true positives. This experiment was performed once.
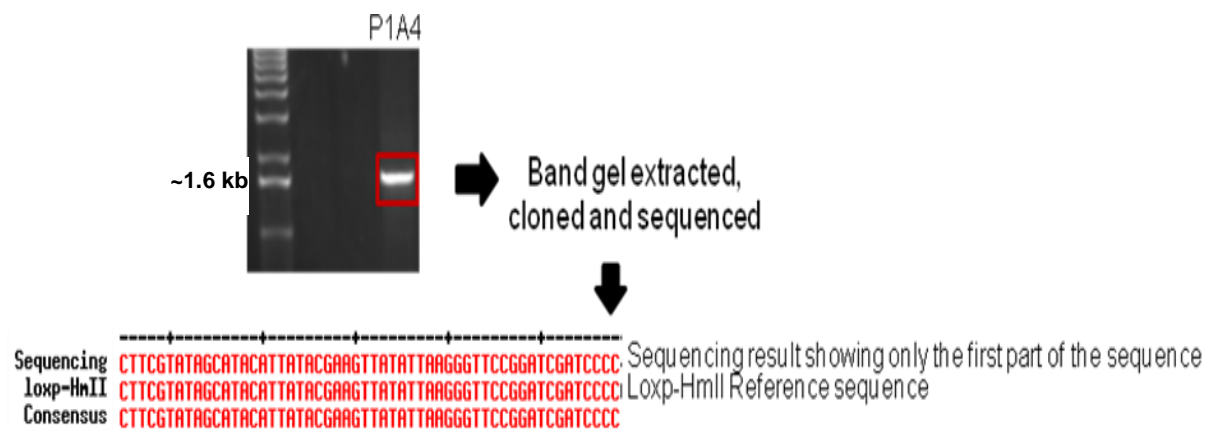
Figure 4.5 Confirmation of the third *loxP* site in the positives using PCR and sequencing

PCR using primers against the *loxP* site and the sequence downstream of HmII was performed with the genomic DNA from P1A4 and P4D3. The PCR product was gel extracted, cloned into pDrive vector and sequenced. The sequence of the PCR amplicon was aligned with the reference *Sash1* sequence using the MultAlin tool. The result confirms the presence of the third *loxP* site.
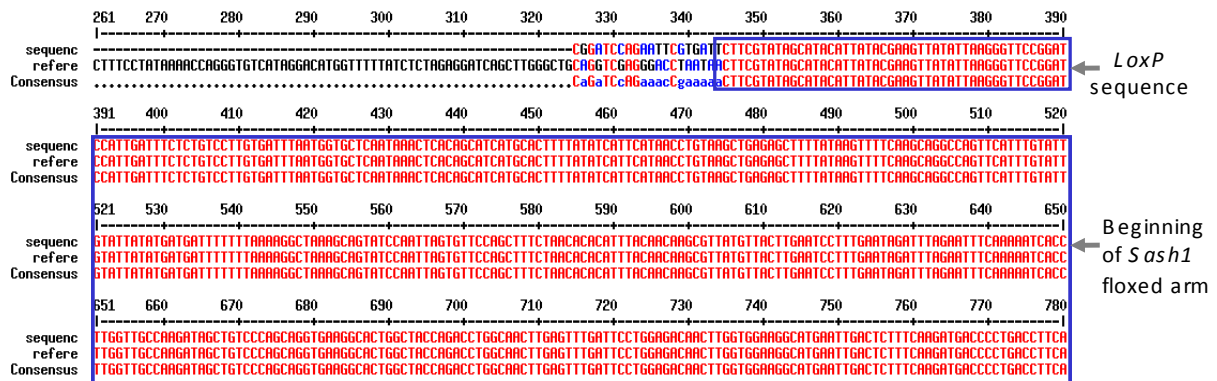
Figure 4.6 Confirmation of the second *loxP* site in the positive clones using PCR and sequencing

PCR using primers against the *loxP* site and the floxed arm was performed with the genomic DNA from the positives. PCR product was gel extracted, cloned into pDrive vector and sequenced. Sequencing result was aligned with the reference *Sash1* sequence using MultAlin tool. Sequencing result confirms the presence of the second *loxP* site.

4.2.5 Removal of the selectable marker from positive ESC

The selectable marker has to be removed before the injection of the ESCs into blastocysts as Thymidine Kinase (TK) causes male sterility in mice. The selectable marker was removed *in vitro* by overexpressing Cre recombinase under a potent promoter, CMV (cytomegalovirus) at the Genetic Modeling Core at BCCA. Figure 4.7 shows the possible outcomes of Cre recombinase overexpression. We performed our first screen using primer set 1 (Figure 4.7), bands of the correct predicted size were found in 8 of 48 clones. These clones were picked for further screening. However, using primer set 2a (Figure 4.7), we could not confirm the presence of the second *loxP* site, but rather the wild-type allele was being amplified. We then performed PCR with primer set 2b (Figure 4.7) to see if we were dealing with total collapse. We could not amplify any band this time. The lack of amplification is most likely technical as we expect amplification of the wild-type allele in either of the total collapse or selectable marker excision scenario. To confirm our initial result, we performed PCR on the same 8 clones with primer set 1 and found no band amplification this time. Thus, the results obtained the first time might have been due to non-specific amplification. We repeated the *in vitro* CMV-Cre overexpression to remove selectable marker in P1A4 and first time in P4D3. However, we did not find any positive clones using primers set 2a and 2b. Based on similar previous work done at the transgenic facility, we might be dealing with a total collapse scenario hence the lack of amplification. However, we need to design new primer sets to overcome the technical challenges.
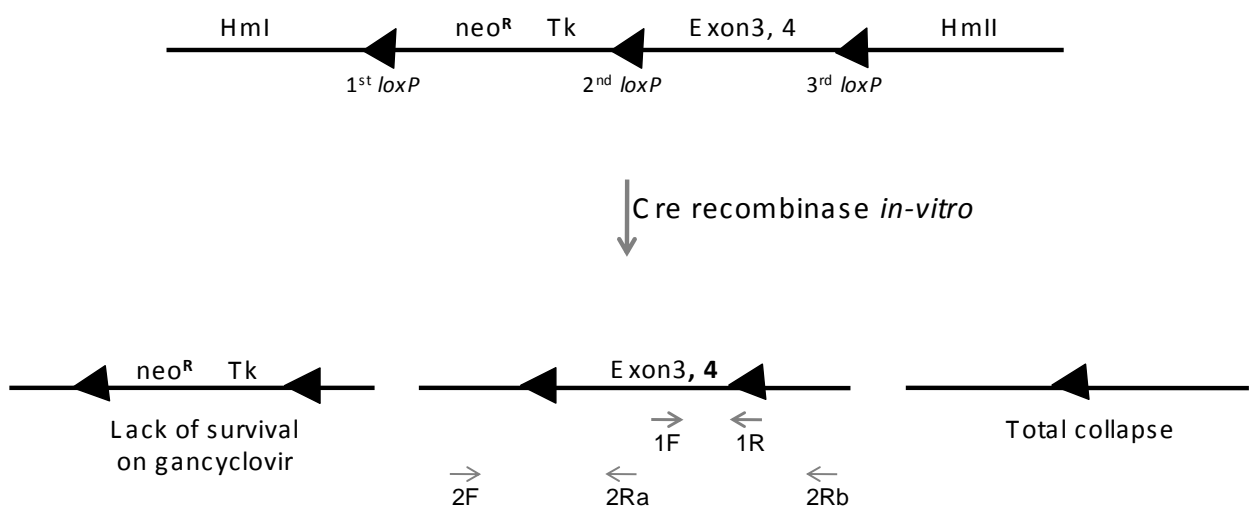
Figure 4.7 The outcomes of the selectable marker removal and the PCR screening strategy

Removal of the selectable marker results in three scenarios as shown in the figure. Overexpression of Cre recombinase could result in the excision of the selectable marker cassette, the floxed arm or both arms. However, the presence of TK in the selectable marker cassette will result in death of ESC clones containing the TK cassette in the presence of gancyclovir in culture. To distinguish between the desired outcome and a total collapse, a PCR screen was used.

4.3 DISCUSSION

We have generated SASH1 floxed-ESC. . The selectable marker cassette has to be removed before ESC injection into blastocysts. To circumvent and troubleshoot the difficulties we are having in removal of the selectable marker, we could try performing the removal with Cre under a different promoter than CMV (cytomegalovirus) or under a different expression level of Cre in culture to find the optimal level of Cre expression. One could either use an inducible Cre system or a system where the expression of Cre is induced in a ligand-dependent manner. Alternative targeting vectors also exist that use the Flp-*frt* system for selectable marker cassette and Cre-*loxP* system for the gene of interest. The Flp-*frt* system however has relatively low efficiency in mammalian cells because of thermolability at physiological temperature [67]. Conditional knock-out mouse models allow spatial or temporal control of the expression of the transgene that are essential for mouse development. However, generating conditionally targeted mice takes time.

After the removal of the selectable marker, ESC would be injected into blastocysts to obtain chimeras. Once the chimeras are obtained, they would be crossed to C57Bl/6J mice and the progeny genotyped for SASH1$^{flox/+}$. Our lab has already generated a VEC-Cre (VEC-Cadherin-driven Cre) strain, which drives endothelial cell-specific expression of Cre recombinase (unpublished data). VEC-Cre and SASH1$^{flox/+}$ mice would be crossed to generate VEC-CRE$^{/-}$; SASH1$^{flox/+}$ mice. This line would then be crossed to SASH1$^{flox/flox}$ to generate endothelial cell-restricted SASH1-null mice (EC-SASH1^{null}). However, if the endothelial cell specific knock-out is lethal then the floxed line could be crossed to an inducible endothelial-specific Cre line such as End-SCL-Cre mice [68] or VE-Cre^{ERT} mice [69].

CHAPTER 5: SUMMARY AND FUTURE PERSPECTIVES

5.1 THE STUDY OF TLR SIGNALING

Since their discovery, TLRs have received much attention and are now the best-studied innate immune receptors against invading pathogens. Despite extensive research in the field of TLRs, our knowledge of the new players in the field is still expanding. Indeed, broadening our understanding of how TLRs function is important in developing targeted therapies beneficial for patients suffering from inflammatory diseases.

We recently found SASH1 to act as a scaffold protein in positively regulating TLR4 signaling pathway by independently interacting with TRAF6/TAK1/IKKβ resulting in activation of NF-κB and subsequent production of proinflammatory cytokines in endothelial cells. (Dauphinee et al., manuscript submitted).

Scaffold molecules can usually play a dual role in signaling pathways. β-arrestin-1 and β-arrestin 2 have been shown as negative regulators of TRAF6 ubiquitination [54]. Interestingly, our lab has confirmed the interaction of SASH1 with both β-arrestin 1 and β-arrestin 2, but whether this interaction is important in regulation of TRAF6 ubiquitination is currently under investigation in our lab. It will be interesting, but not surprising, to identify SASH1 playing a dual role in activation of TLR4 pathway as it will further our understanding of SASH1 function in addition to understanding how our body has mechanisms regulating innate immune responses.

5.2 SUMMARY AND FUTURE DIRECTIONS: THE ROLE OF SASH1 DURING DEVELOPMENT *IN VIVO*

As discussed in chapter 3, the homozygous gene-trap pups die perinatally. We did not detect any obvious difference in the liver, heart and brain of SASH1 homozygous gene-trap and those of wild-type. However, a thorough investigation of all the organs should be performed to characterize SASH1 homozygous gene-trap mice. Our preliminary results show that the lungs of the homozygous gene-trap are not inflated and sink in PBS. Lack of lung inflation could be due to a developmental defect or surfactant deficiency in the lungs or due to a defect somewhere else that controls respiration. In order to conclusively investigate the lung defect, morphometric analysis of the lungs should be performed. The lung, like a sponge, changes its volume according to the external pressure. Therefore, analysis of the airway size and measurement of the areas and volumes should be done relative to a certain total lung volume. The lung should be fixed in inflation to a total lung capacity of about 25 cm water pressure (25 Pascals). Frozen lungs are inflated with OCT or low melting agarose before fast freezing. Mathematical models are used to determine size and shape of airways and alveoli [70]. Cellularity in the lung could be studied using either the *in situ* method with specific staining of cells or by cell extraction followed by specific staining and fluorescent-activated cell sorting (FACS). Staining using cell-type specific antibodies could be beneficial in analysis of defect in the specific cell population of the lung. This will help in identifying the expression pattern of SASH1 during development. Depending on which cell population is affected, players of known developmental pathways could be investigated for identification of the underlying mechanism.

Development of the airways and mesenchyme in the lung is tightly controlled and coordinated. Airway branching occurs at the same time as vascular development. After branching is complete, capillary beds form around alveoli in the mesenchyme. Normal lung

development depends on interactive signaling between the epithelial cells and mesenchymal cells of the lung [16]. For example, the mesenchymal cells produce FGF family members that are crucial for epithelial cells development, while epithelial cells produce Shh and BM4 important for mesenchymal development [16]. SASH1 is predominantly expressed in the endothelium in the lungs of the adult heterozygous gene-trap mice (Dauphinee et al., manuscript submitted). Thus, if we assume an endothelial-specific SASH1 expression during embryonic development, then an epithelial specific defect in the homozygous gene-trap lungs could be due to an impairment in the interactive signaling between the endothelial and epithelial cells. VEGF, an endothelial growth factor, is expressed in epithelial cells, while its receptors are expressed on endothelial cells in the developing lung [19]. Inhibition of VEGF results in inhibition of not only vascular development, but also of airways [19]. VEGF has been shown to be upregulated by LPS; and VEGF expression in macrophages has been shown to be regulated by NF-κB. A study done by Kiriakidis S et al. showed that LPS-induced production of VEGF in human macrophages were almost completely inhibited (>90%) following overexpression of IκBα [71]. Thus, it will be important to compare the expression levels of VEGF and its receptors in SASH1 homozygous gene-trap lungs compared to that in the wild-type lungs.

It should be noted that one of the main functions of the endothelial cells at birth is to reduce PVR so that alveolar fluid is cleared and blood can transit through the lungs for the first time [15]. One way endothelial cells do that is by producing vasodilators such as nitric oxide. It is possible that SASH1 homozygous gene-trap endothelial cells are impaired in the process of nitric oxide production or another vasodilator, hence the lack of respiration. Lack of inflation could be also due to surfactant deficiency or decreased function [17].

TLR4 is expressed on epithelial cells and mesenchymal cells of the lungs during development [72]. Activation of TLR4 inhibits FGF10 resulting in abnormal saccular airway morphogenesis [73]. LPS, the ligand for TLR4, has also been reported to prevent normal branching and elongation of the airways by inhibiting expression of FGF-10 and BMP4. However, in the current study, SASH1 gene-trap mice are not stimulated with LPS. Ubiquitous NF-κB has been shown to be involved in directing branching morphogenesis in the developing chick lung [74]. In this study, high level expression of *RelA* was found in the non-branching mesenchyme, but not in epithelial cells. Inhibition of NF-κB in mesenchyme increased epithelial growth and budding, thus the authors concluded that normally mesenchymal NF-κB inhibits epithelial growth and branching in the embryonic chick lung model. Changes in NF-κB activity also affected expression of genes important in branching morphogenesis such as *Fgf10* and *Bmp4* [74]. Overexpression of the RelA subunit of NF-κB in lung epithelial cells results in increased alveolar type I and type II cells [75]. Moreover, NF-κB activity is shown to correlate with VEGF mRNA expression as inhibition of NF-κB activity decreases VEGF mRNA expression in MDA-MB-231 cancer cells [76]. It is interesting, however, that IL-6, a pro-inflammatory cytokine induced by NF-κB, has opposite effect to that of ubiquitous NF-κB. Increased IL-6 enhances lung maturation and airway budding [77]. However, it should be noted that IL-6 is expressed in the epithelial cells of the lung. IL-6 knock-outs show a halt in neovascularization in a lung model of angiogenesis [78]. These findings further demonstrate that lung development depends on tight developmental coordination between epithelial and endothelial cells. However, it should be also considered that the role of SASH1 during development could be independent of its role in the TLR4 pathway in the adult mice.

To confirm the SASH1 gene-trap mouse phenotype, we have created a second gene-trap mouse that has the insertion of the β-geo construct within intron 2-3 of SASH1 gene. This results in the loss of all functional domains. This second line will be analyzed for neonatal death seen in the first line.

5.3 SUMMARY AND FUTURE DIRECTIONS: THE ROLE OF ENDOTHELIAL SASH1 IN LPS SIGNALING/ LPS-INDUCED SEPSIS

TLR4 signaling is crucial in induction of the hyperinflammatory response and tissue injury during sepsis. Members of TLR4 pathway have been shown to play important roles in LPS signaling. IRAK4$^{-/-}$ mice show resistance to lethal dose of LPS [34]. MyD88$^{-/-}$ mice show improved survival in a model of polymicrobial sepsis [46]. Systemic hyperinflammatory reaction is attenuated, but is not absent in MyD88$^{-/-}$ animals. Production of cytokines and chemokines are inhibited in the lungs and livers of MyD88$^{-/-}$ mice, but not in their spleen during sepsis, suggesting that a MyD88-independent pathway is favored in splenocytes. TRAF6 knockdown results in reduced expression of pro-inflammatory cytokines upon LPS stimulation [62], while TRAF6 knock-out mice die embryonically or prenatally due to a CNS defect [79].

The endothelium plays an important role in mediating the early hyperinflammatory response in sepsis by releasing inflammatory mediators, recruiting leukocytes and facilitating their transmigration into tissue and vasoregulation [9]. Thus, it is crucial to understand the molecular changes that take place in endothelial cells during sepsis as the phenotypic changes are a result of alteration in the expression of endothelial specific genes. A study by Ye *et al*. showed that endothelial-specific blockade of NF-κB, using a mutant IκBα, resulted in inhibition of the adhesion molecules expression, decreased production of NO, reduced neutrophil infiltration, systemic hypotension and in coagulation events [11]. However, these mice did not show a

significant difference in clearing bacteria compared to wild-type mice. These studies show that the endothelium plays a specific role in the pathogenesis of sepsis.

The ability to selectively manipulate endothelial gene expression *in vivo* allows us to clearly define the role of individual endothelial specific gene in a specific disease phenotype. Thus, studying innate immune signaling genes, primarily expressed in endothelium, by generating endothelial-specific gene knock-out mice will further our understanding of the importance of the endothelium in response to LPS *in vivo*. Indeed, we aimed to generate SASH1 floxed-ESC to make endothelial-specific SASH1 knock-out mice. We generated two ESC clones having floxed allele of SASH1 with the help of the Genetic Modeling Core at BCCA as shown in Chapter 4. We floxed SASH1 exon 3 and 4 to generate a stop codon in exon 5 when floxed region is excised through Cre recombination. Our lab is currently working on making these mice.

Endothelial-specific SASH1 knock-out mice will be an ideal system to study the role of endothelial SASH1 in the innate immune response to LPS or Gram-negative sepsis. Since SASH1 promotes endothelial TLR4 signaling, which is important in sepsis, we hypothesize that SASH1 endothelial-specific deletion will block or reduce the effects of endotoxemia. In these studies, SASH1-null mice would be tested for (i) leukocyte recruitment by testing for expression of endothelial adhesion molecules E-selectin, ICAM-1 and vascular adhesion molecule (VCAM) in the lung, heart and liver of the mice; (ii) neutrophil infiltration in the lungs, heart, liver, kidney and intestine by H&E staining; (iii) tissue injury by histopathological examination of the lungs, liver and kidney sections; and (iv) systemic hypotension by measuring the blood pressure of the mice. Based on the hypothesis above, one would expect lower expression of adhesion molecules, less neutrophil infiltration, lower tissue injury, close to normal blood pressure and lower pro-

inflammatory cytokines levels in SASH1 endothelial knock-outs compared to wild-type LPS-treated mice.

5.4 GENERAL SUMMARY

This thesis is a continuation and addition to the recent findings in our lab that identified SASH1 as a novel regulator of TLR4 in endothelial cells. Key experiments in the first part of this thesis confirm the role of SASH1 as a positive regulator of the pathway by promoting activation of NF-κB in endothelial cells. We also showed that SASH1 does not directly interact with Uev1A and Ubc13 suggesting that SASH1 does not induce TRAF6 ubiquitination by directly binding to the E2 ligases, but that the E2 ligases are incorporated into a complex by binding TRAF6 and each other. The finding that SASH1 does not interact with the regulatory subunit IKKγ of IKK complex also adds to our understanding of the protein binding partners of SASH1 as a scaffold protein in TLR4 signaling. Data presented in the first part of this thesis also demonstrate that homozygosity for the *Sash1* gene-trap allele results in perinatal lethality and provides preliminary analysis of the lung as a potential organ being affected by the SASH1 disrutpion. The work in the second part of this thesis generates SASH1 floxed ESC to make endothelial SASH1 knock-out mice. Thus, the work in this thesis begins characterizing SASH1 homozygous gene-trap mice phenotype and it has also begun the process of generating endothelial-specific SASH1-null mice to study the role of SASH1 in response to LPS hence contributing to the field of innate immune signaling.

REFERENCES

1.   Dudley, D.J., *The immune system in health and disease.* Baillieres Clin Obstet Gynaecol, 1992. **6**(3): p. 393-416.

2.   Gallo, R.L. and V. Nizet, *Innate barriers against infection and associated disorders.* Drug Discov Today Dis Mech, 2008. **5**(2): p. 145-152.

3.   Van den Abbeele, P., et al., *The host selects mucosal and luminal associations of coevolved gut microorganisms: a novel concept.* FEMS Microbiol Rev, 2011. **35**(4): p. 681-704.

4.   Ehrnthaller, C., et al., *New insights of an old defense system: structure, function, and clinical relevance of the complement system.* Mol Med, 2011. **17**(3-4): p. 317-29.

5.   Groves, E., et al., *Molecular mechanisms of phagocytic uptake in mammalian cells.* Cell Mol Life Sci, 2008. **65**(13): p. 1957-76.

6.   Cruvinel Wde, M., et al., *Immune system - part I. Fundamentals of innate immunity with emphasis on molecular and cellular mechanisms of inflammatory response.* Rev Bras Reumatol, 2010. **50**(4): p. 434-61.

7.   Lundy, D.J. and S. Trzeciak, *Microcirculatory dysfunction in sepsis.* Crit Care Clin, 2009. **25**(4): p. 721-31, viii.

8.   Dauphinee, S.M. and A. Karsan, *Lipopolysaccharide signaling in endothelial cells.* Lab Invest, 2006. **86**(1): p. 9-22.

9.   Volk, T. and W.J. Kox, *Endothelium function in sepsis.* Inflamm Res, 2000. **49**(5): p. 185-98.

10.   Rittirsch, D., M.A. Flierl, and P.A. Ward, *Harmful molecular mechanisms in sepsis.* Nat Rev Immunol, 2008. **8**(10): p. 776-87.

11.   Ye, X., et al., *Divergent roles of endothelial NF-kappaB in multiple organ injury and bacterial clearance in mouse models of sepsis.* J Exp Med, 2008. **205**(6): p. 1303-15.

12.   Vallet, B., *Bench-to-bedside review: endothelial cell dysfunction in severe sepsis: a role in organ dysfunction?* Crit Care, 2003. **7**(2): p. 130-8.

13.   Bannerman, D.D., M. Sathyamoorthy, and S.E. Goldblum, *Bacterial lipopolysaccharide disrupts endothelial monolayer integrity and survival signaling events through caspase cleavage of adherens junction proteins.* J Biol Chem, 1998. **273**(52): p. 35371-80.

14.   Warburton, D., et al., *Lung development and susceptibility to chronic obstructive pulmonary disease.* Proc Am Thorac Soc, 2006. **3**(8): p. 668-72.

15.   Wojciak-Stothard, B. and S.G. Haworth, *Perinatal changes in pulmonary vascular endothelial function.* Pharmacol Ther, 2006. **109**(1-2): p. 78-91.

16.   El-Hashash, A.H., et al., *Six1 transcription factor is critical for coordination of epithelial, mesenchymal and vascular morphogenesis in the mammalian lung.* Dev Biol, 2011. **353**(2): p. 242-58.

17.   Weaver, T.E. and J.A. Whitsett, *Function and regulation of expression of pulmonary surfactant-associated proteins.* Biochem J, 1991. **273(Pt 2)**: p. 249-64.

18.   van Tuyl, M., et al., *Role of oxygen and vascular development in epithelial branching morphogenesis of the developing mouse lung.* Am J Physiol Lung Cell Mol Physiol, 2005. **288**(1): p. L167-78.

19.   Zhao, L., et al., *Vascular endothelial growth factor co-ordinates proper development of lung epithelium and vasculature.* Mech Dev, 2005. **122**(7-8): p. 877-86.

20.   Takeda, K. and S. Akira, *TLR signaling pathways.* Semin Immunol, 2004. **16**(1): p. 3-9.

21. Lu, Y.C., W.C. Yeh, and P.S. Ohashi, *LPS/TLR4 signal transduction pathway.* Cytokine, 2008. **42**(2): p. 145-51.

22. Lauw, F.N., D.R. Caffrey, and D.T. Golenbock, *Of mice and man: TLR11 (finally) finds profilin.* Trends Immunol, 2005. **26**(10): p. 509-11.

23. Wu, H., et al., *Expression patterns and functions of toll-like receptors in mouse sertoli cells.* Endocrinology, 2008. **149**(9): p. 4402-12.

24. O'Neill, L.A., *The interleukin-1 receptor/Toll-like receptor superfamily: 10 years of progress.* Immunol Rev, 2008. **226**: p. 10-8.

25. Takeda, K. and S. Akira, *Toll-like receptors in innate immunity.* Int Immunol, 2005. **17**(1): p. 1-14.

26. Barton, G.M., J.C. Kagan, and R. Medzhitov, *Intracellular localization of Toll-like receptor 9 prevents recognition of self DNA but facilitates access to viral DNA.* Nat Immunol, 2006. **7**(1): p. 49-56.

27. Kopp, E. and R. Medzhitov, *Recognition of microbial infection by Toll-like receptors.* Curr Opin Immunol, 2003. **15**(4): p. 396-401.

28. Tsan, M.F. and B. Gao, *Endogenous ligands of Toll-like receptors.* J Leukoc Biol, 2004. **76**(3): p. 514-9.

29. Beg, A.A., *Endogenous ligands of Toll-like receptors: implications for regulating inflammatory and immune responses.* Trends Immunol, 2002. **23**(11): p. 509-12.

30. Poltorak, A., et al., *Defective LPS signaling in C3H/HeJ and C57BL/10ScCr mice: mutations in Tlr4 gene.* Science, 1998. **282**(5396): p. 2085-8.

31. Dunzendorfer, S., et al., *TLR4 is the signaling but not the lipopolysaccharide uptake receptor.* J Immunol, 2004. **173**(2): p. 1166-70.

32. Wright, S.D., *CD14 and innate recognition of bacteria.* J Immunol, 1995. **155**(1): p. 6-8.

33. Arditi, M., et al., *Endotoxin-mediated endothelial cell injury and activation: role of soluble CD14.* Infect Immun, 1993. **61**(8): p. 3149-56.

34. Suzuki, N., et al., *Severe impairment of interleukin-1 and Toll-like receptor signalling in mice lacking IRAK-4.* Nature, 2002. **416**(6882): p. 750-6.

35. Naito, A., et al., *Severe osteopetrosis, defective interleukin-1 signalling and lymph node organogenesis in TRAF6-deficient mice.* Genes Cells, 1999. **4**(6): p. 353-62.

36. Lamothe, B., et al., *The RING domain and first zinc finger of TRAF6 coordinate signaling by interleukin-1, lipopolysaccharide, and RANKL.* J Biol Chem, 2008. **283**(36): p. 24871-80.

37. Kobayashi, T., M.C. Walsh, and Y. Choi, *The role of TRAF6 in signal transduction and the immune response.* Microbes Infect, 2004. **6**(14): p. 1333-8.

38. Mendoza, H., et al., *Roles for TAB1 in regulating the IL-1-dependent phosphorylation of the TAB3 regulatory subunit and activity of the TAK1 complex.* Biochem J, 2008. **409**(3): p. 711-22.

39. Kishida, S., et al., *TAK1-binding protein 2 facilitates ubiquitination of TRAF6 and assembly of TRAF6 with IKK in the IL-1 signaling pathway.* Genes Cells, 2005. **10**(5): p. 447-54.

40. Kanayama, A., et al., *TAB2 and TAB3 activate the NF-kappaB pathway through binding to polyubiquitin chains.* Mol Cell, 2004. **15**(4): p. 535-48.

41. Deng, L., et al., *Activation of the IkappaB kinase complex by TRAF6 requires a dimeric ubiquitin-conjugating enzyme complex and a unique polyubiquitin chain.* Cell, 2000. **103**(2): p. 351-61.

42. Chen, Z.J., *Ubiquitin signalling in the NF-kappaB pathway.* Nat Cell Biol, 2005. **7**(8): p. 758-65.

43. Wang, C., et al., *TAK1 is a ubiquitin-dependent kinase of MKK and IKK.* Nature, 2001. **412**(6844): p. 346-51.

44. Scheidereit, C., *IkappaB kinase complexes: gateways to NF-kappaB activation and transcription.* Oncogene, 2006. **25**(51): p. 6685-705.

45. Chen, Z., et al., *Signal-induced site-specific phosphorylation targets I kappa B alpha to the ubiquitin-proteasome pathway.* Genes Dev, 1995. **9**(13): p. 1586-97.

46. Kawai, T., et al., *Unresponsiveness of MyD88-deficient mice to endotoxin.* Immunity, 1999. **11**(1): p. 115-22.

47. Doyle, S., et al., *IRF3 mediates a TLR3/TLR4-specific antiviral gene program.* Immunity, 2002. **17**(3): p. 251-63.

48. Hoshino, K., et al., *Differential involvement of IFN-beta in Toll-like receptor-stimulated dendritic cell activation.* Int Immunol, 2002. **14**(10): p. 1225-31.

49. Yamamoto, M., et al., *Role of adaptor TRIF in the MyD88-independent toll-like receptor signaling pathway.* Science, 2003. **301**(5633): p. 640-3.

50. Oganesyan, G., et al., *Critical role of TRAF3 in the Toll-like receptor-dependent and -independent antiviral response.* Nature, 2006. **439**(7073): p. 208-11.

51. Hacker, H., et al., *Specificity in Toll-like receptor signalling through distinct effector functions of TRAF3 and TRAF6.* Nature, 2006. **439**(7073): p. 204-7.

52. Zhande, R., et al., *FADD negatively regulates lipopolysaccharide signaling by impairing interleukin-1 receptor-associated kinase 1-MyD88 interaction.* Mol Cell Biol, 2007. **27**(21): p. 7394-404.

53. Boone, D.L., et al., *The ubiquitin-modifying enzyme A20 is required for termination of Toll-like receptor responses.* Nat Immunol, 2004. **5**(10): p. 1052-60.

54. Wang, Y., et al., *Association of beta-arrestin and TRAF6 negatively regulates Toll-like receptor-interleukin 1 receptor signaling.* Nat Immunol, 2006. **7**(2): p. 139-47.

55. Shaw, A.S. and E.L. Filbert, *Scaffold proteins and immune-cell signalling.* Nat Rev Immunol, 2009. **9**(1): p. 47-56.

56. Zeller, C., et al., *SASH1: a candidate tumor suppressor gene on chromosome 6q24.3 is downregulated in breast cancer.* Oncogene, 2003. **22**(19): p. 2972-83.

57. Rimkus, C., et al., *Prognostic significance of downregulated expression of the candidate tumour suppressor gene SASH1 in colon cancer.* Br J Cancer, 2006. **95**(10): p. 1419-23.

58. Beer, S., et al., *Impaired immune responses and prolonged allograft survival in Sly1 mutant mice.* Mol Cell Biol, 2005. **25**(21): p. 9646-60.

59. Zhu, Y.X., et al., *The SH3-SAM adaptor HACS1 is up-regulated in B cell activation signaling cascades.* J Exp Med, 2004. **200**(6): p. 737-47.

60. Wang, D., et al., *Enhanced adaptive immunity in mice lacking the immunoinhibitory adaptor Hacs1.* FASEB J, 2010. **24**(3): p. 947-56.

61. Triantafilou, M., et al., *Mediators of innate immune recognition of bacteria concentrate in lipid rafts and facilitate lipopolysaccharide-induced cell activation.* J Cell Sci, 2002. **115**(Pt 12): p. 2603-11.

62. Liu, S., et al., *TRAF6 knockdown promotes survival and inhibits inflammatory response to lipopolysaccharides in rat primary renal proximal tubule cells.* Acta Physiol (Oxf), 2010. **199**(3): p. 339-46.

63. Wooff, J., et al., *The TRAF6 RING finger domain mediates physical interaction with Ubc13.* FEBS Lett, 2004. **566**(1-3): p. 229-33.

64. Li, M.O., et al., *Phosphatidylserine receptor is required for clearance of apoptotic cells.* Science, 2003. **302**(5650): p. 1560-3.

65. Weighardt, H., et al., *Cutting edge: myeloid differentiation factor 88 deficiency improves resistance against sepsis caused by polymicrobial infection.* J Immunol, 2002. **169**(6): p. 2823-7.

66. Jaisser, F., *Inducible gene expression and gene modification in transgenic mice.* J Am Soc Nephrol, 2000. **11 Suppl 16**: p. S95-S100.

67. Utomo, A.R., A.Y. Nikitin, and W.H. Lee, *Temporal, spatial, and cell type-specific control of Cre-mediated DNA recombination in transgenic mice.* Nat Biotechnol, 1999. **17**(11): p. 1091-6.

68. Gothert, J.R., et al., *Genetically tagging endothelial cells in vivo: bone marrow-derived cells do not contribute to tumor endothelium.* Blood, 2004. **104**(6): p. 1769-77.

69. Monvoisin, A., et al., *VE-cadherin-CreERT2 transgenic mouse: a model for inducible recombination in the endothelium.* Dev Dyn, 2006. **235**(12): p. 3413-22.

70. Bolender, R.P., D.M. Hyde, and R.T. Dehoff, *Lung morphometry: a new generation of tools and experiments for organ, tissue, cell, and molecular biology.* Am J Physiol, 1993. **265**(6 Pt 1): p. L521-48.

71. Kiriakidis, S., et al., *VEGF expression in human macrophages is NF-kappaB-dependent: studies using adenoviruses expressing the endogenous NF-kappaB inhibitor IkappaBalpha and a kinase-defective form of the IkappaB kinase 2.* J Cell Sci, 2003. **116**(Pt 4): p. 665-74.

72. Prince, L.S., et al., *Toll-like receptor signaling inhibits structural development of the distal fetal mouse lung.* Dev Dyn, 2005. **233**(2): p. 553-61.

73. Benjamin, J.T., et al., *FGF-10 is decreased in bronchopulmonary dysplasia and suppressed by Toll-like receptor activation.* Am J Physiol Lung Cell Mol Physiol, 2007. **292**(2): p. L550-8.

74. Muraoka, R.S., et al., *Mesenchymal expression of nuclear factor-kappaB inhibits epithelial growth and branching in the embryonic chick lung.* Dev Biol, 2000. **225**(2): p. 322-38.

75. Londhe, V.A., et al., *NF-kB induces lung maturation during mouse lung morphogenesis.* Dev Dyn, 2008. **237**(2): p. 328-38.

76. Shibata, A., et al., *Inhibition of NF-kappaB activity decreases the VEGF mRNA expression in MDA-MB-231 breast cancer cells.* Breast Cancer Res Treat, 2002. **73**(3): p. 237-43.

77. Nogueira-Silva, C., et al., *IL-6 is constitutively expressed during lung morphogenesis and enhances fetal lung explant branching.* Pediatr Res, 2006. **60**(5): p. 530-6.

78. Nogueira-Silva, C., et al., *Intrinsic catch-up growth of hypoplastic fetal lungs is mediated by interleukin-6.* Pediatr Pulmonol, 2008. **43**(7): p. 680-9.

79. Lomaga, M.A., et al., *Tumor necrosis factor receptor-associated factor 6 (TRAF6) deficiency results in exencephaly and is required for apoptosis within the developing CNS.* J Neurosci, 2000. **20**(19): p. 7384-93.